2014

Factors Affecting Storm Characteristics in the Battery and Vicinity

Shannon A. Kay
University of North Florida, s.kay.98096@unf.edu

FACTORS AFFECTING STORM CHARACTERISTICS IN THE BATTERY AND VICINITY

By

Shannon Ariel Kay

A thesis submitted to the School of Engineering is partial

fulfillment of the requirements for the Master of Science in Civil Engineering

UNIVERSITY OF NORTH FLORIDA

COLLEGE OF COMPUTING, ENGINEERING AND CONSTRUCTION

May, 2014

The thesis "Factors Affecting Storm Characteristics in the Battery and Vicinity" submitted by Shannon Kay in partial fulfillment of the requirements for the degree of Master of Science in Civil Engineering has been approved by
The thesis committee: Date:

_____ _____
Donald T. Resio, PhD

_____ _____
Nicholas Hudyma, PhD

_____ _____
Peter Bacopolous, PhD

Accepted for the School of Engineering:

_____ _____
Dr. Murat Tiryakioglu, PhD, CQE
Director of the School of Engineering

Accepted for the College of Computing, Engineering, and Construction:

_____ _____
Dr. Mark Tumeo, PhD, PE
Dean of the College of Computing, Engineering, and Construction

Accepted for the University:

_____ _____
Dr. Len Roberson, PhD
Dean of the Graduate School

ACKNOWLEDGEMENT

First and foremost, I would like to thank my committee chair and friend Professor Donald Resio. I will forever appreciate the time and effort you put into teaching me about natural hazards, a field I have become so passionate about. I hope that one day my research will surpass the level you expect from me so that you know your time and guidance was not wasted. Next I would like to thank another committee member, Professor Nicholas Hudyma, who helped me get to where I am today. Without your guidance I may not have went to graduate school and found my passion. I sometimes do not understand the faith you two have in me, but the pressure drives me to be the best I can, and that I will not forget.

I would like to thank Joseph Leffler for his support and sacrifice during my studies as well as the love he gave that keep me going. I would also like to thank my grandmother, Janice Owen for the faith and love that will always touch my heart; I hope to make you proud. Also, thank you to the rest of my family for the support and love you gave me while I have been in college.

CONTENTS

LIST OF TABLES vii

LIST OF FIGURES ix

ABSTRACT xi

CHAPTER 1 INTRODUCTION 1

CHAPTER 2 HISTORICAL PERSPECTIVE 7

2.1 HAZARD ASSESSMENTS DEVELOPED FOR THE BAV 7

2.2 RELATIONSHIP BETWEEN SEA SURFACE TEMPERATURE (SST) AND INTENSITY 8

2.3 RELATIONSHIP BETWEEN ATMOSPHERIC CIRCULATION AND TC FREQUENCY 8

CHAPTER 3 DATA 11

CHAPTER 4 METHODOLOGY 15

4.1 METHODOLOGY OF PART ONE: INVESTIGATION OF VARIABILITY OF LARGE-SCALE PRESSURE PATTERNS, SST AND ASSOCIATED VARIATION IN STORM CHARACTERISTICS 16

4.2 METHODOLOGY OF PART 2: EVALUATION OF PARAMETER RELATIONSHIPS RELATIVE TO HAZARD ESTIMATES 25

4.2.1 TESTING FOR DIFFERENT STORM INTENSITIES WITH ANGLE TRAVELED 25

4.2.2 TESTING A RELATIONSHIP BETWEEN CENTRAL PRESSURE AND FORWARD VELOCITY 28

4.2.3 METHODOLOGY OF PROBABILITY CALCULATIONS OF SANDY AND IRENE 28
4.2.4 INVESTIGATING THE GOODNESS OF FIT OF STORM OCCURRENCES TO THE POISSON DISTRIBUTION 30
CHAPTER 5 RESULTS OF PART 1: THE ANALYSIS OF FACTORS AFFECTING STORM FREQUENCY AND INTENSITY 32
5.1 IDENTIFYING A RELATIONSHIP BETWEEN ATMOSPHERIC PRESSURE AND TC's 32
5.2 OBSERVING THE DATA IN A SINGLE VARIABLE TABLE 34
5.3 DETERMINING A RELATIONSHIP BETWEEN STORM FREQUENCIES AND MULTIPLE FACTORS 35
5.4 TESTING FOR A RELATIONSHIP BETWEEN THE SIGNIFICANT EOFS AND SST 38
5.5 REEVALUATING CONTINGENCY TABLES INCLUDING THE EFFECTS OF CORRELATION BETWEEN SST AND EOFs 41
5.6 TESTING A RELATIONSHIP BETWEEN STORM HEADING AND WEIGHTING 44
5.7 DISCUSSION OF THE RELATIONSHIP OF CLIMATE AND TROPICAL CYCLONES 45
CHAPTER 6 RESULTS OF PART 2: EVALUATION OF PARAMETER RELATIONSHIPS RELATIVE TO HAZARD ESTIMATES 52
6.1 STORM INTENSITY VS. ANGLE 52
6.2 RELATIONSHIP BETWEEN CENTRAL PRESSURE AND FORWARD VELOCITY 56
6.3 HAZARDOUS STORM DISTRIBUTION 57

6.4 PROBABILITIES OF SANDY AND IRENE 60

6.5 DISCUSSION OF CURRENT HAZARD ESTIMATES FOR TROPICAL CYCLONES 61

CHAPTER 7 CONCLUSION 63

REFERENCES 65

APPENDIX A 68

APPENDIX B 77

VITA 83

LIST OF TABLES

Table 1: Storm Characteristic Probability Parameters (FEMA 2012) 4

Table 2: Tropical Storm Data Set Used in the Investigation of Climate Relationships 13

Table 3: Storm Frequencies per Category of Weightings 20

Table 4: Contingency Table of Multiple Weighting's effect on Storm Frequencies 21

Table 5: Chi-Squared Critical Values (Dougherty 2001) 22

Table 6: SST/ Weighting Contingency Table for Years with Storm 22

Table 7: Critical Values for Pearson's test of Linear Regression (R-value) 23

Table 8: Student's t-Distribution Critical Values (Dougherty 2001) 26

Table 9: Contingency Table Comparing a Theoretical Exponential Distribution of the Time Between TC Events to the Actual number of Occurrences 31

Table 10: Single Variable Tables of W3 34

Table 11: Single Variable Tables of W7 35

Table 12: Single Variable SST Tables 35

Table 13: Weightings 3 vs. SST Contingency Tables 36

Table 14: Weighting 7 vs. SST Contingency Table 36

Table 15: Weighting of EOF3 vs. Weighting of EOF7 38

Table 16: Expected Probabilities within the Contingency Table for EOF3 and SST 42

Table 17: Expected Probabilities within the Contingency Table for EOF7 and SST 42

Table 18: Contingency Table of SST and EOF3 with Revised X^2 Based on Linear Relationship 43

Table 19: Contingency Table of SST and EOF7 with Revised X^2 Based on Linear Relationship 43

Table 20: Contingency Table of Storm Angle and Weighting of EOF6 44

Table 21: Central Pressure Statistics by Direction 53

Table 22: Contingency Table of Frequency of All Storms Observed Compared to Theoretical Exponential Frequency 59

Table 23: Contingency Table of PDF of Intense Storms Compared to Theoretical Exponential Distribution 60

Table 24: Probabilities of the Individual Parameters of Sandy and Irene 61

Table 25: Contingency Table of Intense Storms' Distribution if the Data were Doubled 62

LIST OF FIGURES

Figure 1a and 1b: New York City in the Aftermath of Hurricane Sandy (Cameron 2012; Minchillo 2012) 2

Figure 2: New York Bight (NYC 2009) 3

Figure 3: Water Levels at the Battery (NOAA 2013) 3

Figure 4: Storm Track Sets Differentiated by Color (FEMA 2012) 5

Figure 5: Map of NYC Coast to Display Line Storms Must Cross to be Included in Dataset 12

Figure 6: Study Approach 15

Figure 7: Illustration of Averaging Procedure 17

Figure 8: Weighting of EOF3 vs Year 33

Figure 9: Weighting 3 vs. SST for each Year 39

Figure 10: Weighting 7 vs. SST for each Year 39

Figure 11: Weighting of EOF3 vs Weighting of EOF7 41

Figure 12: Contours of EOF(7) Showing Semi-Permanent Circulation Aspects 46

Figure 13: Contours of EOF 3 Showing Semi-Permanent Circulation Aspects 47

Figure 14: 1938 Storm Track and Sea Surface Pressure (Byers 1944) 48

Figure 15: Contours of EOF(6) Showing Semi-Permanent Circulation Aspects 49

Figure 16: Seasonal, Time-Centered, Five-Year Average SST at Battery Park 50

Figure 17: Histogram of Storm Angles 52

Figure 18: Angle of Direction vs. Central Pressure 54

Figure 19: Gumbel Ranking for Central Pressures Differentiated by Angles 55

Figure 20: Return Period of Central Pressure based on Storm Angle 56

Figure 21: Forward Velocity vs. Surface Pressure Regression..... 57

Figure 22: Frequency of Time Between All Observed Storms Compared to Theoretical Poisson 58

Figure 23: Observed Frequency of Time Between Intense Storms Compared to Theoretical Poisson Frequency 59

ABSTRACT

Tropical cyclones (TCs) Irene and Sandy caused major damages in back to back years to the most densely populated city in the United States stunning the residents with storms linked to seemingly impossible probabilities. Such activity has raised questions about the effect of non-stationary aspects within atmospheric circulation on storm behavior and some assumptions inherent in previous hazard studies of the New York City (NYC) area. This study analyzes statistical aspects of hazard quantification for this area related to this non-stationarity and statistical characterization. In particular this study investigates the presence of multiple populations of storms, it also tests current assumptions inherent in these previous studies which produce surge hazards which differ significantly and it investigates a natural relationship between storm characteristics and large scale climate variations through Empirical Orthogonal Functions (EOF) of the sea surface pressure.

The findings of this study show that there is a statistically significant influence of climate variability on storm frequency, intensity and direction within the Battery and vicinity (BAV, Battery Park and surrounding region). Variations in large-scale atmospheric pressure patterns as well as sea surface temperature appear to be significantly affecting the surge hazard for this region.

This study also shows there is a statistically significant relationship between storm heading and intensity as well as the presence of multiple populations of storms driven by different atmospheric states that behave with alternate characteristics. These multiple populations appear to be significantly influencing the overall average of storm behavior causing inaccurate assumptions in hazard quantification which leads to misestimation in risks.

CHAPTER 1 INTRODUCTION

In recent years, there has been a growing knowledge and acceptance that coastal risks are increasing around the world. This heightened risk perception particularly hits home for the United States after all of the catastrophic events caused by hurricanes along its coastal regions (i.e. Katrina, Sandy, Ike, Francis, etc.). Before these recent events, many researchers would have deemed them relatively impossible. In spite of all these recent events, it seems as though a disaster always seems to surprise the inhabitants of the area it strikes. The National Hurricane Center states that the "Atlantic is in a period of heightened activity that started around 1995 and could last at least another decade" (Goldenberg et al 2001). Most recently, the most densely populated city in the U.S., New York City, was impacted by these Atlantic TCs in back to back years by Irene (2011) and Sandy (2012), which both caused devastating surge levels. In the NYC area, storm characteristics over the last few years have dramatically exceeded the expected frequency and intensity. These two extreme events prompted the formation of The Rockefeller Commission. This effort was initiated in order to develop a comprehensive resilience strategy for NYC to decrease the amount of time NYC needs to recover industrially and economically after tropical events (Rodin et al 2013). A successful resilience strategy requires fully understanding what risks could arise and what, if anything, is causing the risk to increase and decrease. Further investigation is required in order to accomplish this goal.

New York City is chosen as our study area because it is an important financial center, a major transportation hub, and is one of the most densely populated areas of the United States. The worldwide economy is dependent on this area and suffers greatly when the stock market is

closed for even one day (Sandy caused a two day closure). Figure 1a depicts a part of the NYC subway system following Sandy; New York was forced to stop all subway transportation as well as shutting down all other means of public transportation, which the city depends on because of its large population. Figure 1b shows the Ground Zero construction site with seawater rushing into it. Sandy and Irene both left many inundated areas and halted many means of communications for the city which impacted the residents of not only New York, but the rest of the United States as well. In addition to the various impacts of Sandy, she was estimated to cause 6.5 billion dollars in damages to the city.

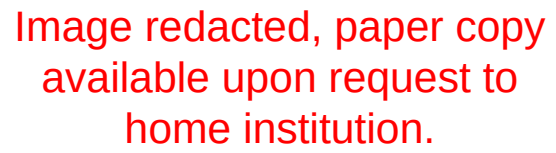

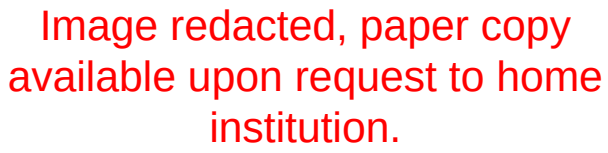

Figure 1a and 1b: New York City in the Aftermath of Hurricane Sandy (Cameron 2012; Minchillo 2012)

NYC is not only economically at risk, but also geographically vulnerable. Storm surge is the most detrimental impact of a tropical cyclone (TC) and this region possesses a coastal geometry (displayed in Figure 2 below) which produces a much higher surge (NYC 2009). This area is also going to become more vulnerable in the future due to the observed sea level rise which is trending upward about 2.77 mm/year (NOAA 2012). Thus, the passage of time will lead to increased flood hazard by this increase in water height depicted in Figure 3. Specifically this

work will focus on the Battery and surrounding vicinity (BAV) because of its central location and proximity to important NYC features.

Figure 2: New York Bight (NYC 2009)

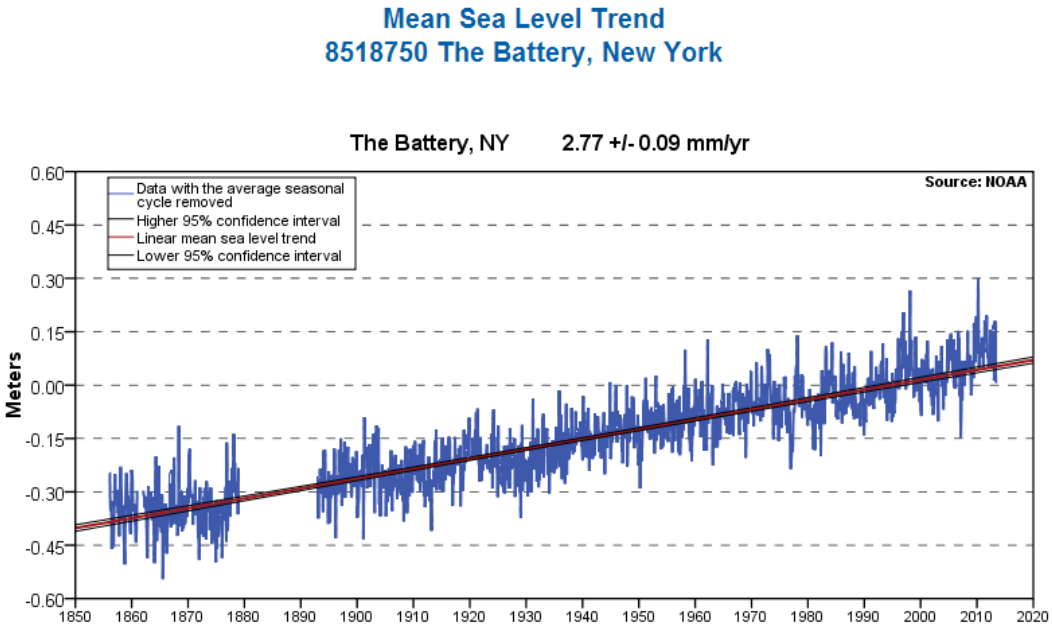

Figure 3: Water Levels at the Battery (NOAA 2013)

Sandy and Irene are both associated to highly unlikely probabilities as discussed further in Chapter 6 Section 4 which are calculated based on the most recent probabilities of storm

characteristics developed for the New York Area by FEMA in 2011 and put into effect in 2012 (FEMA 2012). The probability of these two storms occurring in back to back years is so incredibly unlikely that it might be considered almost impossible. There are two main reasons as to why there are highly improbable events in short periods of time that are discussed below in the following three paragraphs. Table 1 displays probability parameters of five dimensions of the storm probability and the associated distributions (FEMA 2012).

Table 1: Storm Characteristic Probability Parameters (FEMA 2012)

Five Dimensional Probability			
Parameter	Distribution	Distribution Parameters	
ΔP (mb)	Truncated Weibull	U=41.1	K=2.05
Rp (km)	Lognormal	med: $\ln(RMW)=3.015-(6.291*10^{-5}\Delta p^2)+0.337\psi$	$\sigma_{lnRp}=0.44$
Vf(kt)	Normal	mean= $6+0.4*\Delta p$	$\sigma=7$
Θ	Normal	mean=22	$\sigma=10$
B (Holland's B)	Normal	mean=1.1	$\sigma=0.2$

The recent, frequent events of high intensity may just be an anomaly, or they may be hinting at an underlying interconnectivity between nature and storm characteristics which is producing an episodic variation in TC hazard that is being overlooked by standard statistics. This is a problem dealing with complex statistics of natural phenomenon while assuming there is no organization in nature, and can be an extremely difficult issue to correct. Hurricane probabilities are calculated assuming secular variation, which can ignore the misunderstood coupling present within natural phenomenon. These variations need to be investigated to determine if they are playing an important role in storm behavior because risk mitigation is contingent upon knowledge of relationships in nature and inclusion of these relationships within hazard calculations. Many studies have linked episodic nature in storm characteristics to the episodic

variations of large scale circulation (or climate variation) in the form of oscillations to storm frequency for different regions, as discussed further within the historical perspective.

Another possibility is the statistics used in current FEMA hazard calculations may be neglecting multiple populations within the storms affecting the BAV which may each exhibit different storm behaviors. The FEMA analysis shows three different tracks that storms tend to follow illustrated in Figure 5 differentiated by colors. Within these tracks, storms may exhibit different characteristics because they are storms of a different type which would create a need for differentiating dependent parameters and calculating relationships based on the multiple sets. If storm are behaving differently, the statistics will misestimate the hazard for the region, making it impossible to properly mitigate the risks associated. Although this study will likely not unveil everything behind natural statistics of tropical storm characteristics for the BAV, it can present methods to test them for other locations and use the information attained to calculate more accurate storm hazard, greatly assisting the resilience effort.

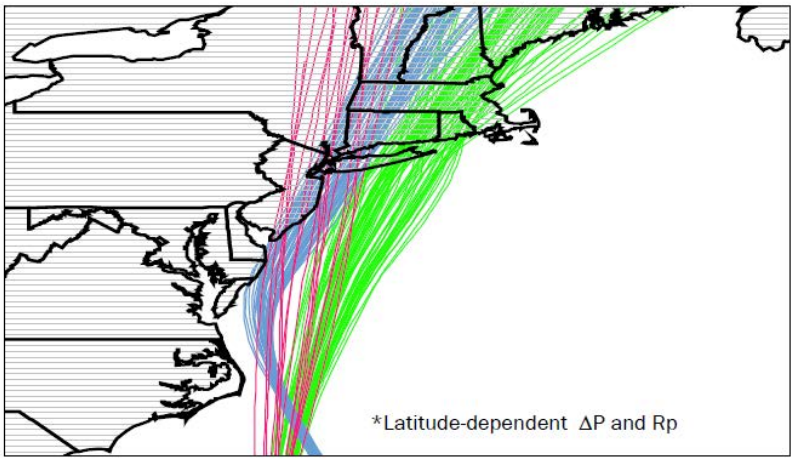

Figure 4: Storm Track Sets Differentiated by Color (FEMA 2012)

The purpose of this thesis is to enhance the knowledge and understanding of tropical cyclone (TC) behavior in the BAV with respect to natural variations through time and with respect to the assumption of homogeneity in storm populations to improve the way natural statistics are dealt with for this area. This study first investigates a relationship between the episodic variations of large scale circulation and storm frequency and storm intensity to determine the role of nature's organization at different scales and its impact on storm surge and phenomenon for the BAV. It next investigates a presence of different populations of storms within the dataset based on angle as well as investigating various assumptions made in calculating currently utilized storm hazards for the BAV. Details describing the steps and motivation behind steps taken are presented within the methodology. A discussion of the results and future work are located at the end of this thesis.

CHAPTER 2 HISTORICAL PERSPECTIVE

The historical perspective first presents previous studies which relate to hazards for this region and the associated methods used. This chapter next discusses findings of previous studies which indicate a need for further investigation of these influences within the BAV.

2.1 HAZARD ASSESSMENTS DEVELOPED FOR THE BAV

Currently the Stephens Institute is investigating surge hazard for the NYC area employing a method of synthetic storms. Hwang (2013) also is investigating storm surge for the area using the Battery water height data from 1920 to 2012 and claims the data follows the generalized extreme value (GEV) distribution with a mean of 8.10ft and COV of 10.07%. He used only the water maxima for this investigation and included every type of event. Lin et al applied a model-based risk assessment methodology by coupling a statistical/deterministic hurricane model with the SLOSH surge model to generate a large amount of synthetic surge events which predicts a surge of Sandy's height to occur about once every 500 years, and a surge of Gloria's height to occur once every 400 years (Lin et al 2010). In the last 200 years three storms surpassed Gloria's surge height which leaves four events in this period to have surges above this estimate of 2.56m. The United States Army Corps of Engineers also conducted a study of Fire Island to Montauk Point (FIMP), but the information from the study was never released.

The item all of these studies fails to address is a possibility of a variable hazard which will be investigated here in this thesis. The National Hurricane Center (NHC) introduces the hypothesis

that TC frequencies are attributed to multi-decadal climate variability, yet there are no studies which investigate the relationship between storm frequencies and surface pressures (which control a great portion of climate variability) (NOAA NHC 2013). "20th Century Reanalysis" was formed for the Atmospheric Circulation Reconstructions over the Earth (ACRE) initiative and is readily available (Compo et al 2011). With the hypothesis by NOAA and the data available, it now seems pertinent to assess the relationship.

2.2 RELATIONSHIP BETWEEN SEA SURFACE TEMPERATURE (SST) AND INTENSITY

A TC is a textbook example of a Carnot (heat) engine (Emanuel 1987). These systems use heat for energy; therefore it is apparent that their strength or intensity is dependent on the amount of heat present in the region of the storm. Warm upper-ocean features can significantly impact TC intensity by providing a positive feedback and cause a sudden increase in intensity while in warm, oceanic regimes (Shay et al 2000). It has also been found that there is a direct correlation between the power dissipation index (PDI) developed by Emanuel (quantifies storm intensity, duration, and frequency) and SST with a 99% certainty in the tropical Atlantic where the storms are forming. The best correlation was shown for a filtered variability on time scales of a few years in order to remove high frequency fluctuations (Emanuel 2007). This evidence suggests a multi-year, non-secular variation that is affecting the SST and therefore the TC intensity within the study region.

2.3 RELATIONSHIP BETWEEN ATMOSPHERIC CIRCULATION AND TC FREQUENCY

There have been many studies linking different pressure oscillations (i.e. North Atlantic Oscillation, El Nino Southern Oscillation) to TC frequencies. HuiJun et al (2007) documented a relationship with the North Pacific Oscillation and Western Pacific TC frequency). There are also studies which even link the Antarctic Oscillation and the Western North Pacific Typhoon

frequencies (Wang and Fan 2004). An negative correlation exists between the El Nino Southern Oscillation and storm frequency within the Atlantic. Also, during years which winds blow from a westerly direction and become more westerly with time there is a substantial increase in TC frequency within the region (Gray 1984). The oscillations around the globe assist or deter TC frequency and should therefore be investigated with a closer look for individual regions. It is hypothesized here that rather than one specific named oscillation controlling TC frequency for each region, the overall atmospheric circulation causes variations in storm frequency and should be analyzed objectively using empirical orthogonal functions (EOF). This thesis will investigate a relationship between the orthogonal functions of variance of the sea surface pressure patterns surrounding the study region and the hurricane frequency.

Throughout the world, with New York not being exempt, large scale climate variations couple with the TC's internal dynamics to determine the TC tracks (Wang et al 2011). The Atlantic Warm Pool as well as the Atlantic Multidecadal Oscillation have been shown to affect storm activity in the Atlantic Basin (Wang et al 2011, Goldenberg et al 2001). There have been many studies conducted which link inter-annual climatology with TC tracks in the North Altantic (eg. Xie et al 2005, Kossin et al 2010). Although these studies exist, there is a lack of studies which focus on a specific region and identify the patterns which induce storm frequency for the region specifically.

Resio and Orelup (2007) conducted a study of climactic variations in TC characteristics which discovered a significant relationship between storms characteristics (mainly surge potential) and Empirical Orthogonal Functions (EOF's). EOF's were utilized here to distinguished natural

patterns in the atmosphere. These patterns were then compared with storms of the Gulf of Mexico and proved to show significant relationships (Resio and Orelup, 2007). This thesis will use similar methodology to investigate relationships between the EOF's developed for the BAV and storm characteristics for this region comparing to all pressure patterns present.

This chapter presents results of previous studies which may relate to this study. Thus, this thesis will investigate the influences presented throughout the historical perspective and their role in TC hazards for the BAV to determine if the hazards are neglecting the influence of the organization in nature.

CHAPTER 3 DATA

There are three major datasets used within this study: 1) TC data including central pressure, angle traveled and forward velocity, 2) Gridded sea level pressure data and 3) Sea surface temperature at Battery Park, N.Y. This chapter will discuss the datasets in further detail to present how and why they were formed and used here.

The TC data used in this study is majorly from the Hurdat2 Reanalysis (HURDAT2 2013), but some of the data came from NWS 38 (NOAA 1987). The TCs used in this dataset along with their maximum central pressure within the study region are shown below in Table 2. To be included in the dataset, the storms must have passed through the 45degree line from 36.5˚N to 41.5˚N and 76˚W to 71˚W off the coast of NYC that is shown in Figure 5; if the TC's track was above this region it was included in the dataset. This filtering was done to eliminate the large amount of bypassing storms of weak nature that pose little threat to the vicinity and will only lower the expected hazards for this region, lessening the ability to mitigate.

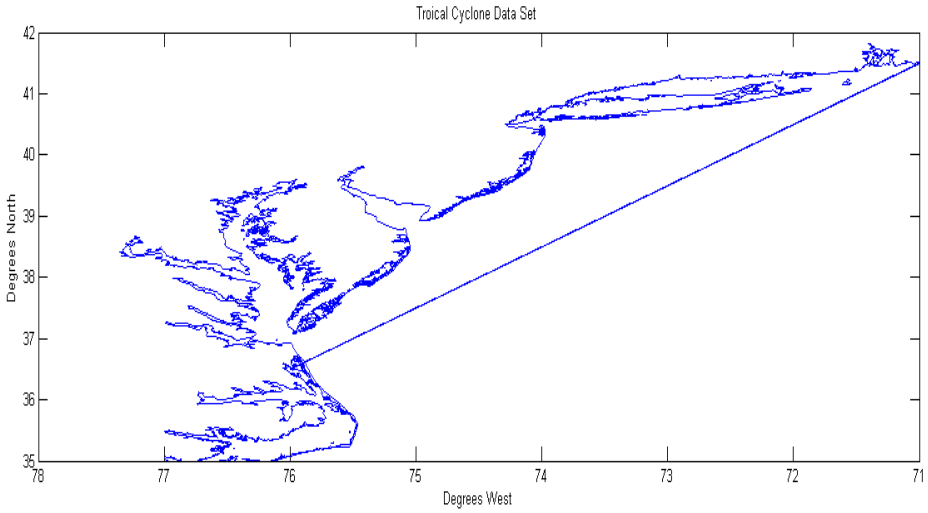

Figure 5: Map of NYC Coast to Display Line Storms Must Cross to be Included in Dataset

Storms referred to as 'intense' throughout this study will be all storms with central pressures 980 and below. The central pressures (Cp) used in this set are only the minimum Cp that the storm exhibits while within the boxed region because that is what affects the BAV. This study also uses the location, angle of incidence, and radius to wind data also available within HURDAT2.

Table 2: Tropical Storm Data Set Used in the Investigation of Climate Relationships

Storm	Max Cp (mb)	Name	Storm	Max Cp (mb)	Name
AL041877	X	Unnamed	AL031954	976	Carol
AL021879	979	Unnamed	AL021955	969	Connie
AL061881	X	Unnamed	AL051960	970	Donna
AL041882	X	Unnamed	AL061961	X	Unnamed
AL021886	X	Unnamed	AL091971	997	Doria
AL041893	X	Unnamed	AL021972	980	Agnes
AL111893	X	Unnamed	AL071976	977	Belle
AL051894	X	Unnamed	AL091985	951	Gloria
AL031897	X	Unnamed	AL101985	1006	Henri
AL061900	X	Unnamed	AL051986	990	Charley
AL041903	990	Unnamed	AL031991	964	Bob
AL011907	X	Unnamed	AL081999	980	Floyd
AL021908	X	Unnamed	AL112000	1005	Gordon
AL011916	990	Unnamed	AL012001	1004	Allison
AL031916	993	Unnamed	AL022004	1012	Bonnie
AL071934	989	Unnamed	AL032004	1014	Charley
AL061938	941	Unnamed	AL232005	1005	Twenty-Two
AL071943	X	Unnamed	AL022007	991	Barry
AL031944	X	Unnamed	AL092011	958	Irene
AL071944	966	Unnamed	AL182012	943	Sandy
AL111944	X	Unnamed			

The mean sea level pressure data used in this study is from the 20th Century Reanalysis which was made available in 2010 after being formed using state-of-the-art data assimilation systems and surface pressure observations (PRMSL 2012). It contains six-hourly, four-dimensional global atmospheric dataset spanning from 1871 to 2012 which covers the entire globe with a two degree by two degree grid. The dataset used in this case is the surface pressure at mean sea level. Only a portion of this set is used for this analysis; this portion is described further below in the methodology.

The sea surface temperature used throughout this study is the temperature retrieved from the Battery tide gauge (8518750) in degrees Celsius (NOAA 2013). A computer program written using Fortran calculates the average SST for the time period between July and October which is used for this study. This data is then smoothed to determine a five-year time centered average that represents yearly variability.

CHAPTER 4 METHODOLOGY

The ultimate goal of this study is to investigate the interrelationships among the large-scale atmospheric variability inherent in this scale of motion and synoptic-scale events, specifically, TCs, to determine if a correlation exists which can be used to produce a hazard for the region with this information. Figure 6 shows this goal in the form of a diagram often used by meteorologists in "down-scaling" studies. The diagram illustrates how each item relates to one another in their different scales and the form of the data which will be compared to one another. The climate variability will be quantified via multivariate analysis of large-scale circulations and synoptic information comes from HURDAT2 and NWS38. Storm surges will be inferred through scaling relationships (Irish and Resio 2010). The methodology of this flow chart and analysis are described below throughout this chapter.

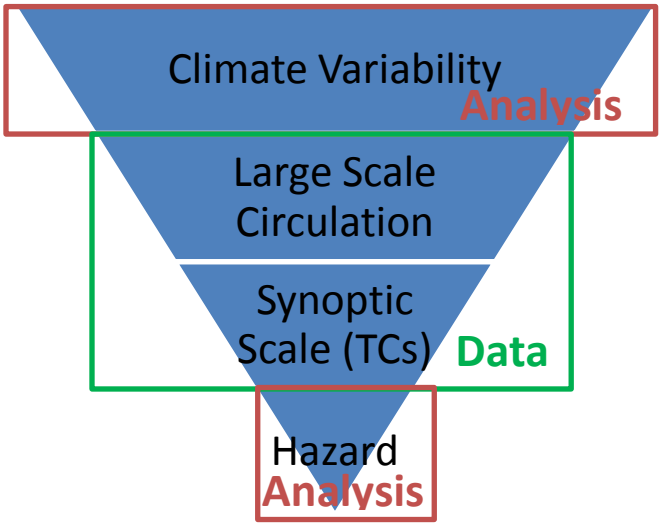

Figure 6: Study Approach

Work in this thesis is divided into two parts: Part 1) Investigation of variability of large-scale pressure patterns, SST and associated variation in storm characteristics and Part 2) Evaluation of parameter relationships relevent to hazard estimation. The methodology of each of these parts will be described throughout this chapter.

4.1 METHODOLOGY OF PART ONE: INVESTIGATION OF VARIABILITY OF LARGE-SCALE PRESSURE PATTERNS, SST AND ASSOCIATED VARIATION IN STORM CHARACTERISTICS

The first step of this investigates relationships between tropical cyclone (TC) behavior and large-scale circulation patterns. To quantify the variation of large-scale patterns, a number of steps were taken employing the surface pressure data from the 20th Century Reanalysis (Compo 2011). To focus on the area of intent, the field is narrowed and utilizes just the area between latitudes of 2-60 degrees N and longitudes of 270-358 and 0-20 degrees E at every two degrees. To filter some of the synoptic scale contribution to the field, input data is averaged onto four degree increments rather than retaining the initial two degree basis. The pressure at the center of four points is calculated by taking the average of the surrounding four points:

$$P_{ijky} = \left(\sum_{i'=2i-1}^{2i} \sum_{j'=2j-1}^{2j} P_{i'j'ky}\right)/4.0 \quad \text{Equation 1}$$

where P is the surface pressure at (i, j), and time, k (k goes from 1-1460 for non-leap years and 1-1464 for leap years), during year, y. Each point is only included in one average. Figure 7 depicts a small set of the points included in the study at every two degrees and the new points at every four degrees to clarify the procedure. It should be noted that each procedure described throughout the methodology section is conducted through computer programs written in Fortran 90 by the author of this thesis, Shannon Kay.

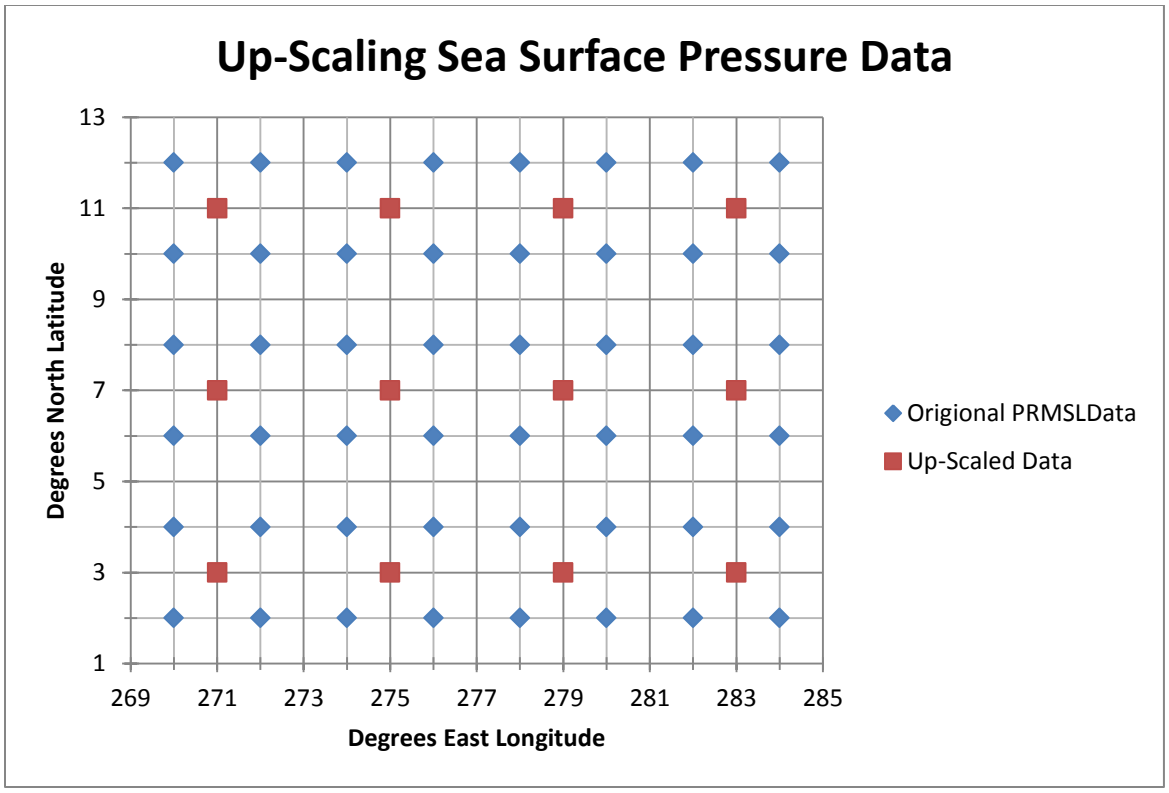

Figure 7: Illustration of Averaging Procedure

These points are then included in calculating five day averages (73 for each year). Each five day average consists of 20 measurements, except for the times of leap year, where 24 measurements are included in the 12th five-day (six days in this case) increment:

$$\overline{P_{ijmy}} = \frac{\left(\Sigma_{k_e}^{k_b} P_{ijky}\right)}{20.0} \quad \text{.....Equation 2}$$

Where,

$$k_b = 20(m-1) + 1 \quad \text{.....Equation 3}$$

$$k_e = 20m \quad \text{.....Equation 4}$$

$$m = int\left(\frac{k-1}{20}\right) + 1 \quad \text{.....Equation 5}$$

An overall average for each of the 73 increments is calculated for the 140 year period from 1871-2010.

$$\overline{P_{ijm}} = \frac{\left(\sum_{y=1}^{140} P_{ijmy}\right)}{140} \quad \text{Equation 6}$$

As shown in Equation 7, a field of pressure deviations from the mean is defined by subtracting the total average for the associated 5-day increment calculated using Equation 6.

$$\Delta P_{ijmy} = \overline{P_{ijmy}} - \overline{P_{ijm}} \quad \text{Equation 7}$$

To characterize the seasonal pressure patterns, the averages of the deviations for the time period from July 29th to November 6th is taken, shown in Equation 8.

$$\overline{\Delta P_{ijy}} = \frac{\left(\sum_{m=42}^{62} \Delta P_{ijmy}\right)}{21} \quad \text{Equation 8}$$

To focus our analysis on multi-year variability, a five year time-centered average is taken from this yearly value, as shown in Equation 9.

$$\overline{\Delta P_{ijy'}} = \frac{\left(\sum_{y=y'-2}^{y'+2} \overline{\Delta P_{ijy}}\right)}{5} \quad \text{Equation 9}$$

The pressure field resulting from this calculation will then be used in computing the covariance matrix. With this methodology, 136 samples are used in the covariance matrix rather than the 140 because the averaging makes it so that two samples are lost on each end. To calculate the covariance matrix, the following equations are used.

$$COV_{LJ} = \frac{\left(\sum_{y=1}^{136} (\Delta P_{Ly} - \overline{\Delta P_L})(\Delta P_{Jy} - \overline{\Delta P_J})\right)}{136} \quad \text{Equation 10}$$

Where L and J are the variable counters in the horizontal and vertical respectively, where both go from one to n, where n is given by:

$$n = (j-1)15 + i \quad \text{Equation 11}$$

From this covariance matrix, eigenvectors are developed which are described in Appendix A. Eigenvectors are orthogonal functions which describe the overall covariance of a data field. These functions can be used to objectively determine states which affect processes occurring

within them, in this case, TC frequency. Here, 15 eigenvectors are estimated which explain descending percentages of the overall variance. A table of the respected variance explained by each empirical orthogonal function (EOF) followed by the plots of each can be found in Appendix A. The eigenfunctions will be referred to throughout this thesis as EOF(n) where n is the number of the eigenvector (1-15).

The results here were generated by the time-centered 5 year average deviations of the 105 day period from July 29th to November 6th, which are the best results to represent variation through time. The running average deviation employs the 105 day period as well as the two 105 day periods surrounding on either side to calculate the time centered average to eliminate randomness and describe multi-year variance. Because many factors contribute to the sea surface pressure, (TCs, small storms, fronts etc.), including them can cause many jagged edges in the output which can overlook the long term behavior of the function. This method smoothes and allows for a better representation of the overall climate variability, ignoring oscillations people are previously acquainted to.

The inner products between thee annual average deviations and EOFs are computed and will be referred to here as the weightings of the EOFs.

$W_{yn} = \sum_{R=1}^{420}(E_{Rn} * \overline{\Delta P_{Ry}})$ ……Equation 12

The weightings provide an accurate representation of the behavior of the pressures and can be used in comparisons to determine potential relationships. Plots of these weightings can be found in Appendix B. For preliminary assessment, the weightings are examined visually for correlation with storm events. All of the weightings are put through the entire relationship testing process,

but it is hypothesized that the ones passing the visual screen will be the ones to show a prominent relationship.

Since the weightings provide a succinct representation of the large-scale circulation, they can be used to define the atmospheric state. Thus each year can be categorized via its weightings on the EOFs and will be used for quantitative analysis to identify which EOFs are affecting TC frequency within the study region. To do this, each of the weightings is first sorted into two groups of equal probability where one group is primarily negative and the other positive. To visualize the effect of the weightings on storm frequency, each will be put into a table, as shown below in Table 3. 'n' represents the number of times a TC occurs during the current weighing's state. If the eigenvector corresponding to its weighting has effect on storms in the area, most of the weightings during that year should be in the same group (either positive or negative), therefore the table values would either ascend or descend. This is conducted once for all storms affecting the BAV and a second time only for intense storms denoted as those with central pressures (Cp) less than or equal to 980 mb to investigate the possibility of effect only during strong events.

Table 3: Storm Frequencies per Category of Weightings

Weighting (1-15)	
$w \leq x$	$w > x$
n	N

The number of storms can then be put into contingency tables similar to Table 3, but including a second weighting in investigate if more than one eigenvector works together to affect storm frequency in the BAV as shown in Table 4.

Table 4: Contingency Table of Multiple Weighting's effect on Storm Frequencies		
Weighting(1-15)	Weighting (1-15)	
	w ≤ x	w > x
w ≤ x	*Data filled in based on the weighting during the year of each storm*	
w > x		

The methodology of testing the statistical significance of these contingency tables can be accomplished through Chi Squared Testing as described below.

Chi Squared Testing

1. Develop a Contingency Table
2. Form Null and Alternative Hypothesis: H_0= No Relationship H_a= A relationship exists
3. Calculate Chi Squared: $X^2 = \sum_{i=1}^{n} \frac{(Observed-Expected)^2}{Expected}$
4. Determine the degrees of freedom
5. Compare to the Critical Value: $X^2 \leq$ Critical Value: Do not reject null hypothesis, $X^2 >$Critical Value: Reject

Since the weightings are split into equal categories, the theoretical expected value for this case is one quarter of the total number of storms because the initial expectation is that there is no relationship and between the weightings and the total number of samples contain equal probability. The critical values used are those at the 95% certainty. The Chi-Squared chart is shown in Table 5.

Table 5: Chi-Squared Critical Values (Dougherty 2001)

χ^2 (Chi-Squared) Distribution: Critical Values of χ^2

	Significance level		
Degrees of freedom	5%	1%	0.1%
1	3.841	6.635	10.828
2	5.991	9.210	13.816
3	7.815	11.345	16.266
4	9.488	13.277	18.467
5	11.070	15.086	20.515
6	12.592	16.812	22.458
7	14.067	18.475	24.322
8	15.507	20.090	26.124
9	16.919	21.666	27.877
10	18.307	23.209	29.588

The contingency tables are also analyzed using only the intense storms to investigate an effect of the EOFs on the frequency of intense storms. Then the EOFs are compared with sea surface temperature (SST) and put into contingency tables where it takes the place of the second weighting, shown in Table 6. This is also done again for only the intense storms.

Table 6: SST/ Weighting Contingency Table for Years with Storm

SST	Weighting (1-15)	
	$w \leq x$	$w > x$
$SST \leq SST_{bar}$	*Data filled in based on the weighting and SST during the year of each storm*	
$SST > SST_{bar}$		

The EOFs are also plotted in a linear regression to investigate a relationship between SST and each eigenvector. Based on the coupling between atmospheric circulation and ocean currents, it is likely that there will be at least one EOF that possesses a significant relationship with SST. The relationship between the weightings on the EOFs and SST will be tested for significance using the Pearson's test of correlation. A table of the critical values for this test along with their associated probabilities is shown below where the probability of significance is (1-α). For this investigation, relationships will be considered significant with a 95% certainty as long as the R value (correlation coefficient) is greater than the critical value shown in the chart corresponding to α of 0.05 where the degrees of freedom for this test are the number of samples minus two.

Table 7: Critical Values for Pearson's test of Linear Regression (R-value)

	One Tailed Probabilities			
Alpha	**0.05**	**0.025**	**0.005**	**0.0005**
	Two-Tailed Probabilities			
N Samples (N-2 DOF)	**0.1**	**0.05**	**0.01**	**0.001**
10	0.549	0.632	0.765	0.872
20	0.378	0.444	0.561	0.679
30	0.306	0.361	0.463	0.57
40	0.264	0.312	0.403	0.501
50	0.235	0.279	0.361	0.451
60	0.214	0.254	0.33	0.414
70	0.198	0.235	0.306	0.385
80	0.185	0.22	0.286	0.361
90	0.174	0.207	0.27	0.341
100	0.165	0.197	0.256	0.324
200	0.117	0.139	0.182	0.231
300	0.095	0.113	0.149	0.189

If a significant relationship exists between EOF and SST, the expected values for the contingency table must then be recalculated to incorporate this correlation into the theoretical expected frequencies. If the newly calculated Chi Squared value is still significant based on 95% certainty and 1 degree of freedom, then it is apparent that the sea surface temperature is working alongside the atmospheric circulation to create an inviting area for tropical storms. The probabilities of frequencies for the expected values are recalculated using Equation 13.

$$F(w,SST) = \int_{x}^{\infty}\int_{SSTbar}^{\infty} \frac{1}{\sqrt{2\pi}\sigma_{SST}} \exp\left(-\frac{(SST-\overline{SST})^2}{2\sigma_{SST}^2}\right) * \frac{1}{\sqrt{2\pi}\sigma_{res}} \exp\left(-\frac{(w-w(SST))^2}{2\sigma_{res}^2}\right) dSSTdw \text{……..}$$

…….....Equation 13

The integral is taken for the various boxes of the contingency table with those values used as the limits where x is the average for each weighting and σ denotes the associated standard deviation. The residual standard deviation for the σ about the linear relationship, w(SST), is calculated using Equation 14

$$\sigma_{res} = \sqrt{1-\rho^2}\sigma_w \text{……..……}$$

Equation 14

where ρ is the correlation coefficient of the line. . The expected value is then calculated for each by:

$$Expected = F(w,SST) * number\ of\ storms \text{ ……..……}$$

Equation 15

Then the X^2 will be reevaluated based on the new expected frequencies.

Contingency tables will be done a final time incorporating storm heading (the angle direction of the storm from the horizontal) where SST was in the table to investigate a relationship between the atmospheric circulation and heading of the storms. Each of the contingency tests will evaluate how the climatic variations are affecting storm characteristics and multiple variations are working together to affect storm frequency and intensity. These results can later be used to

mitigate storm hazards through a better understanding of storm behavior based on the organization in nature.

4.2 METHODOLOGY OF PART 2: EVALUATION OF PARAMETER RELATIONSHIPS RELATIVE TO HAZARD ESTIMATES

The next step of this study is to investigate various assumptions made and test methodology of current hazard estimates. These statistical analyses will test common assumptions and possible relationships for a varying hazard of storms that can be used in a future assessment of hazard for the area.

4.2.1 TESTING FOR DIFFERENT STORM INTENSITIES WITH ANGLE TRAVELED

The first step in this investigation is to determine whether or not there are storms following different behaviors that are related to other identifiable factors. A preliminary screening suggested that storm heading, the angle of direction counter-clockwise from horizontal is affected by storm intensity. Consequently, the storms were divided into two sets either heading less than or equal to 65 degrees, or greater than 65 degrees, which was chosen as the cut off because the two sets have relatively equal probabilities. The means and standard deviations are calculated for the minimum central pressures (Cp) of each of data sets and are compared using a Student's T test to determine if the values are statistically different. The steps of this hypothesis testing are as follows:

1) Form Null and Alternative Hypothesis: H0: M1=M2; Ha: M1≠ M2 where M signifies the mean
2) Calculate student's t: $t = \frac{M_1 - M_2}{\sqrt{\frac{(n_1-1)S_1^2+(n_2-1)S_2^2}{n_1+n_2-2}\left[\frac{n_1+n_2}{n_1 n_2}\right]}}$
3) Determine Degrees of Freedom

4) Compare to the Critical Value: t≤ Critical Value: Do not reject null hypothesis, $t >$Critical Value: Reject (Critical value is determined by t-test statistic with values shown in Table 8.

Table 8: Student's t-Distribution Critical Values (Dougherty 2001)

t Distribution: Critical Values of t

		Significance level					
Degrees of freedom	*Two-tailed test:* *One-tailed test:*	10% 5%	5% 2.5%	2% 1%	1% 0.5%	0.2% 0.1%	0.1% 0.05%
1		6.314	12.706	31.821	63.657	318.309	636.619
2		2.920	4.303	6.965	9.925	22.327	31.599
3		2.353	3.182	4.541	5.841	10.215	12.924
4		2.132	2.776	3.747	4.604	7.173	8.610
5		2.015	2.571	3.365	4.032	5.893	6.869
6		1.943	2.447	3.143	3.707	5.208	5.959
7		1.894	2.365	2.998	3.499	4.785	5.408
8		1.860	2.306	2.896	3.355	4.501	5.041
9		1.833	2.262	2.821	3.250	4.297	4.781
10		1.812	2.228	2.764	3.169	4.144	4.587
11		1.796	2.201	2.718	3.106	4.025	4.437
12		1.782	2.179	2.681	3.055	3.930	4.318
13		1.771	2.160	2.650	3.012	3.852	4.221
14		1.761	2.145	2.624	2.977	3.787	4.140
15		1.753	2.131	2.602	2.947	3.733	4.073
16		1.746	2.120	2.583	2.921	3.686	4.015
17		1.740	2.110	2.567	2.898	3.646	3.965
18		1.734	2.101	2.552	2.878	3.610	3.922
19		1.729	2.093	2.539	2.861	3.579	3.883
20		1.725	2.086	2.528	2.845	3.552	3.850
21		1.721	2.080	2.518	2.831	3.527	3.819
22		1.717	2.074	2.508	2.819	3.505	3.792
23		1.714	2.069	2.500	2.807	3.485	3.768
24		1.711	2.064	2.492	2.797	3.467	3.745
25		1.708	2.060	2.485	2.787	3.450	3.725
26		1.706	2.056	2.479	2.779	3.435	3.707
27		1.703	2.052	2.473	2.771	3.421	3.690
28		1.701	2.048	2.467	2.763	3.408	3.674
29		1.699	2.045	2.462	2.756	3.396	3.659
30		1.697	2.042	2.457	2.750	3.385	3.646

If the mean Cps of each set is statistically different, it is likely that alternate storm tracks denote different storm intensities and these storms may be affected by physical factors related to large-scale atmospheric states. If the TCs have statistically different average intensities, the next step will be to test the relationship between angle and Cp by plotting them against each other and forming a regression. The regression will be tested for significance with the same method described for testing the regression above with Table 7.

Continuing the investigation of the effect of storm angle on intensity, a Gumbel ranking method is used to determine the different estimates, truncating the heading angle with as close to possible equal probabilities. The Gumbel ranking will be done on a plot with each of the two as well as the entire set in one (three lines). This is done by first determining the CDF for each of the storms by sorting from largest to smallest because the higher the Cp denotes a weaker storm.

$F(x) = \frac{Rank}{n+1}$ ……..……Equation 16

Where F(x) is the Cumulative Distribution Function (CDF) and, the rank is the number of the storm after it is put into ascending order of weakest to strongest intensities, and n is the number of storms within the dataset. The next step in the Gumbel ranking process is to take the double log of the equation:

$x = -\ln(-\ln(F(x))$…….……Equation 17

This is then plotted as the x value, and the y value is plotted as the Central pressure. If the two sets trend differently, it is likely that the Cp return period has been misestimated for storm events. The linear trend of this line can be used in estimating return periods of central pressures. The return period for each of these lines will be done using the Poisson frequency (μ) and the regression.

$\mu = \frac{number\ of\ events}{time\ period}$……Equation 18

In this case, the Poisson frequency is 47/162 because during the 162 years from 1851 to 2013, 47 storms crossed into this region.

The expected return period is calculated by:

$T = \frac{1}{\mu(1-F(x))}$ ……..……Equation 19

The double natural log taken for the return period and this value is then entered into the regression equation to find the corresponding Cp.

$Cp = m(\ln(ln(T)) + b$ ……..……..……..Equation 20

Where m is the slope and b is the y intercept of the regression equation. This is then done for a wide range of values to make a plot of the Cp's against their return period. Each of the three sets (the angle above the cut off, angle below, and the set of both is plotted in order to visualize the difference in prediction for the datasets considering separation versus together. This method can identify if central pressure return periods are being misestimated therefore causing hazard calculations to produce incorrect values.

4.2.2 TESTING A RELATIONSHIP BETWEEN CENTRAL PRESSURE AND FORWARD VELOCITY

The relationship between central pressure and forward velocity is tested using a linear regression because the current hazard calculations utilized for the BAV are calculated using a mean Vf linearly dependent on the pressure differential of the TC. A regression of the two will be plotted and the associated correlation coefficient is compared to a critical value of R=0.30 based off 46 degrees of freedom and a 95% certainty.

4.2.3 METHODOLOGY OF PROBABILITY CALCULATIONS OF SANDY AND IRENE

Each parameter probability of Sandy and Irene presented in section 6.4 are calculated using the distributions in Table 1 (FEMA 2012). The probabilities for the parameters following a normal distribution (where x can be Θ and V_f) were calculated using the CDF (cumulative density function) formula for a normal distribution:

$F(x) = \int_0^x \frac{1}{\sigma\sqrt{2\pi}} * e^{\left[\frac{(x-\bar{x})^2}{2\sigma^2}\right]}$ ……..……Equation 21

where σ is the standard deviation and $\bar{x}$ is mean of either Θ or V_f depending on which the probability is being calculated; both are found in Table 1. Although the Holland's B parameter also follows the normal distribution, the associated probabilities for this were not calculated because B shows very little variability in this region for stronger storms. The probabilities for pressure differential (x=ΔP) are calculated based on a truncated Weibull where the exceedance probability is (FEMA 2012):

$$E(x) = \exp\left[-\left(\frac{x}{U}\right)^k + \left(\frac{\Delta P_0}{U}\right)^k\right] \quad \text{Equation 22}$$

Where U and k are constants 41.2 and 2.05 respectively and ΔP_0 is equal to 33mb. The final calculation used in this probability is the lognormal distribution for R_p, the radius to maximum winds. The formula for the median used is taken to be similar to Vickery and Wadhera (2008):

$$m = \ln(R_p) = 3.015 - (6.291 * 10^{-5})\Delta P^2 + 0.0337\psi \quad \text{Equation 23}$$

Where R_p is dependent on latitude, ψ, and the pressure differential. This median is the expected value for the radius to maximum winds used in the lognormal CDF (x=R_p):

$$F(x) = \int_0^x \left(\frac{1}{x*\sigma\sqrt{2\pi}}\right) * exp\left[-\frac{(\ln(x)-\ln(m))^2}{2\sigma^2}\right] \quad \text{Equation 24}$$

The exceedance probability for storms is somewhat more complicated. In a complete multivariate analysis we would have

$$E(z) = 1 - F(z) \quad \text{Equation 25}$$

where

$$F(z) = 1 - (\int\int\int\int\int f(v_f, R_p, \theta, \Delta P, x_0)H(z, \Lambda(v_f, R_p, \theta, \Delta P, x_0))dv_f dR_p d\theta d\Delta p dx_0 \quad \text{Equation 26}$$

This is typically done using a numerical model; however, a complete computer simulation of all possible storms is beyond the scope of this thesis.

4.2.4 INVESTIGATING THE GOODNESS OF FIT OF STORM OCCURRENCES TO THE POISSON DISTRIBUTION

The assumption that storms follow a Poisson distribution is tested by comparing the theoretical exponential distribution of years between storms to the actual distribution of years between storms with a Chi Squared test. The Poisson frequency parameter, λ, is used in the exponential distribution to calculate the expected number of occurrences for the numbers of years between storms. The equation of the CDF for the exponential distribution is as follows:

$F(x) = 1 - e^{-\lambda x}$……..…..……Equation 27

The pdf is:

$f(x) = \lambda e^{-\lambda x}$……..……..…..Equation 28

For this case, λ is equal to 47/162 because 47 storms occurred in the last 162 years within this dataset. To convert the probabilities for the CDF into number of events to compare, the total number of events is multiplied by each value. This number is used to determine the number of events within each category.

$Theoretical\ Events = number\ of\ storms * \int_{X1}^{x2} f(x)\, dx$……..Equation 29

To eliminate the large number of zero values in the contingency table, years will be combined into multiyear increments. For the case of all storms, these increments will consist of four year periods. The contingency table to be filled in based on this information is shown in Table 9.

Table 9: Contingency Table Comparing a Theoretical Exponential Distribution of the Time Between TC Events to the Actual number of Occurrences

	0-3 Y	4-7 Y	8-11 Y	12-15 Y	16-19 Y
Observed	*Data filled in based on the observed frequency and the calculated theoretical frequency (Equation29)*				
Theoretical					

These values are then used to calculate the X^2 test statistic and tested for significance based on four degrees of freedom and 95% certainty. In addition to tests for all storms, this test is repeated for only intense storms to determine if more hazardous storms follow the assumed distribution. The theoretical calculations for intense storms are done based on the Poisson frequency of $\lambda=12/114$. The data from 1900 and on is used for the intense storms because of the large number of data before this period lacking storm central pressure.

The relationships tested throughout this chapter will provide a better understanding of the behavior of tropical cyclones affecting the BAV. This information will provide the foundation for improved hazard quantification for the NYC area.

CHAPTER 5 RESULTS OF PART 1: THE ANALYSIS OF FACTORS AFFECTING STORM FREQUENCY AND INTENSITY

This study identifies important and interesting aspects about storm characteristics which affect the risk for the Battery and vicinity (BAV). As will be shown here, there is at least one atmospheric state which is associated with increased storm frequency and intensity. There is also a correlation between SST and storm frequency for all storms which becomes more significant for intense storms. In a physical context, the atmosphere state and SST provide a means for tropical cyclones to enter the region and remain intense while doing so. This information is evaluated via Chi Squared testing and is presented throughout this chapter.

5.1 IDENTIFYING A RELATIONSHIP BETWEEN ATMOSPHERIC PRESSURE AND TC's

A preliminary investigation, a visual screening of the EOF weightings, identified which conditions in the atmosphere tended to steer TCs into the BAV. If the weighting on an EOF affects storms within the region, it might expected to have opposite deviations (opposite signs) during times of heavy activity compared to during times of inactivity. In the visual screening, EOF3 stood out as one which may have some effect over the storms within the region because of its drastic lows during the times of notable storms within the region, as depicted in Figure 8. This weighting illustrates some striking features; in the period during the 1920's to the early 30's the value is very positive which corresponds to a period of inactivity while the weighting shows some interesting lows during times of intense activity. The 1938 Storm (The Long Island Express/New England Hurricane) occurred during a local minima where the data set is shifting into the negative region, The Great Atlantic Hurricane of 1944 occurred during the first major

low in the data, Donna of 1960 also happened during a local minima, Gloria of 1985 coincided with a distinct dip in weighting, and finally towards the end of the weighting where Irene occurs is intensely negative, yet Sandy occurred during an upward swing in the weighing. This positive feature in 2012 neglects the smoothing done to describe long term variability because the data from 2013 and 2014 was not available and therefore may be different than the output presented. Also, this value may incorporate the behavior of Sandy because she was present for a long period of time during this season. Although all weightings will continue to be analyzed, the focus will be shifted to EOF3 since it appears to have most potential to relate with storms within the region.

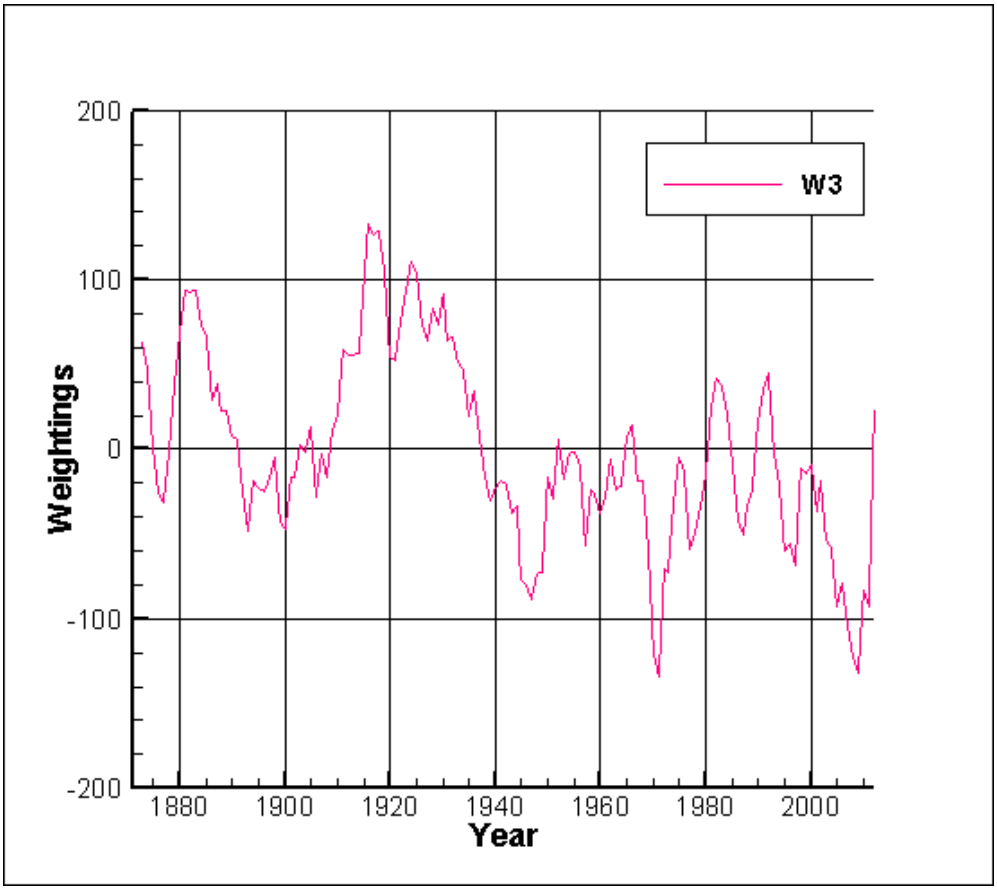

Figure 8: Weighting of EOF3 vs Year

5.2 OBSERVING THE DATA IN A SINGLE VARIABLE TABLE

In order to further understand how much each EOF affects the frequency of storms within the region, each EOF's weightings are placed into a single variable table, where the probability of each year possessing a certain weighting is equal. The number put into the table coincides with a TC occurring in conjuncture with that atmospheric state. If the EOF affects the storm frequency in the BAVs then there should be a trend in the numbers within the tables. These tables are calculated for all storms as well as a second time for only intense storms. If a relationship exists, it is hypothesized that trend will be emphasized when considering only intense storms. This test is another screen and does not present the statistical significance of a relationship, but is a useful tool in solving the puzzle. The tables with the highest trends are shown in tables 10 and 11. Weightings on EOF3 and EOF7 appear to display a pattern which affects TC frequencies. Although all the EOF's will continue to be investigated, it is likely that one or both of these are affecting the steering of storms into the BAV while the atmospheric pressure is being controlled by the opposite (negative) of the EOF. Each table shown below actually contains two tables. The left shows a table for all storms and the right shows a table for only intense storms. The contingency tables throughout this thesis will continue to display two tables into one.

Table 10: Single Variable Tables of W3

Weighting 3			
All Storms		Intense Storms	
$w \leq x$	$w > x$	$w \leq x$	$w > x$
28	13	8	4

Table 11: Single Variable Tables of W7			
Weighting 7			
All Storms		Intense Storms	
$w \leq x$	$w > x$	$w \leq x$	$w > x$
27	14	10	2

The next single variable table made is the number of storms versus the SST; it is done in the same fashion as the tables of the weightings and is shown in Table 12. Although there are many storms in each category for years with storms, the intense storms seem to only be present during times of high SST. This suggests that the intensity of the storm is affected by current SST in the vicinity. This suggests that it is justifiable to continue investigating a relationship between intense storms and SST for the BAV.

Table 12: Single Variable SST Tables			
Sea Surface Temperature			
All Storms		Intense Storms	
$SST \leq SST_{bar}$	$SST > SST_{bar}$	$SST \leq SST_{bar}$	$SST > SST_{bar}$
17	24	1	11

5.3 DETERMINING A RELATIONSHIP BETWEEN STORM FREQUENCIES AND MULTIPLE FACTORS

The next step is to move on to a double variable table and test for statistical significance since it is possible that storm probabilities depend on more than one factor. From a meteorological perspective, it is likely that the atmosphere and the sea contribute to storm frequency in this region as well as the strength of these storms because large-scale atmospheric pressure state strongly influences storm steering and storm intensity is related to SST. It is also possible that

more than one of the EOFs control the large-scale steering currents which drive storms into this region as well as the SST coming into account coupling with the atmosphere and influencing storm frequency. Each weighing on the EOF was put into a double variable table with the others as well as with the SST. The striking tables are shown below along with their calculated Chi-Squared values. In this case Chi-Squared values are determined according to one degree of freedom. In order to have a relationship with 95% significance, the value must be above 3.84. To be significant with 99% certainty, the Chi-Squared value must be above 6.64. ` All of the notable tables presented here possess values at least significant with 99% certainty. There are other tables which have high Chi-Squared values, but the ones displayed here are only those which have both high values in the intense storm years as well as all storm years. Tables for weightings three and seven are the significant ones shown below in Tables 13 and 14.

Table 13: Weightings 3 vs. SST Contingency Tables

Weighting on EOF 3	All Storms		Intense Storms	
	X^2	13.731708	X^2	10.00
	$w \leq x$	$w > x$	$w \leq x$	$w > x$
$SST \leq SST_{bar}$	8	9	1	0
$SST > SST_{bar}$	20	4	7	4

Table 14: Weighting 7 vs. SST Contingency Table

Weighting on EOF 7	All Storms		Intense Storms	
	X^2	18.219511	X^2	22.00
	$w \leq x$	$w > x$	$w \leq x$	$w > x$
$SST \leq SST_{bar}$	6	11	0	1
$SST > SST_{bar}$	21	3	10	1

These two tables are striking because they are both display extremely significant interactions with certainty above 99% when comparing to a critical value of 6.63 therefore majorly affect TC frequency within the BAV. The storms tend to occur in conjunction with higher than average SST's and negative weightings on both the EOF's shown. In addition to the significantly high Chi Squared value, it is has also been seen that the vast majority of the weak storms disappear from the times which there are positive weightings and low SST's (which is shown in the table on the right of intense storms in Tables 13 and 14). The SST seems to be primarily affecting the storm intensity in the BAV and the weightings on the EOFs appear to be more influential on storm frequency. The weightings of EOF3 and EOF7 have also been compared against each other in another contingency table to determine if the two work together to create the proper atmospheric conditions for TC's which can be seen in Table 15. It appears that the two weightings combine to steer TC's into the BAV, and it also appears that when both the EOF's are affecting the pressure positively, that intense storms have little ability to enter the region at all. The EOFs are simply orthogonal functions which represent the covariance of the system based on the entire field, but these two EOFs have similar local features surrounding the BAV which would sensibly combine to steer TCs into this region. These similar local features can be seen in the contours of the EOFs found in Appendix A. This tool allows individuals to identify patterns and relate these patterns with occurrences and in this case, more than one of these patterns relates to TC presence.

Table 15: Weighting of EOF3 vs. Weighting of EOF7					
Weighting of EOF 3					
Weighting of EOF7	All Storms			Intense Storms	
	X^2	9.8292685		X^2	6.666667
		$w \leq x$	$w > x$	$w \leq x$	$w > x$
	$w \leq x$	18	9	6	4
	$w > x$	10	4	2	0

There is statistical evidence with 99% certainty that EOF3 and EOF7 combine to steer TC's into the area because the calculated Chi Squared values are greater than the critical value of 6.63. Because there is a zero in the intense storm table, the result of this analysis is weaker than for tables with no zero's, but it is clear to those viewing the table that a relationship exists concluding that these functions greatly influence storm frequency. When both of the weightings are negative, the probability for a cyclone to enter the BAV is much higher.

The statistical tests performed were based on the expectation of equal probabilities in each of the categories of the table, but if a linear relationship exists between either of the weightings on EOFs and the SST or the two EOFs weightings, then the expected values need to be recalculated based on that and reevaluated for significance. Thus, a test of the relationship between these variables will be conducted in the next section.

5.4 TESTING FOR A RELATIONSHIP BETWEEN THE SIGNIFICANT EOFS AND SST

To confirm the significance of the contingency tables, a relationship EOFs and SST is investigated. A relationship between the weightings on EOF3 and EOF7 is also investigated to confirm significance, although it is unlikely because of the orthoganality constraint of the EOF

estimation. These relationships are tested using linear regressions and are presented in Figures 9-11 .The weightings and SSTs corresponding to the year are shown in these figures below as well as the associated linear equations and the squared values of the correlation coefficients.

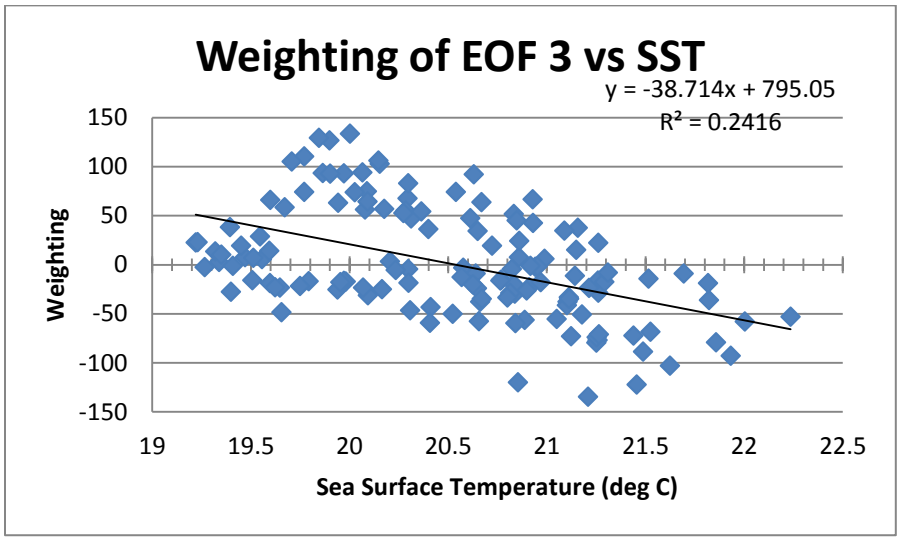

Figure 9: Weighting 3 vs. SST for each Year

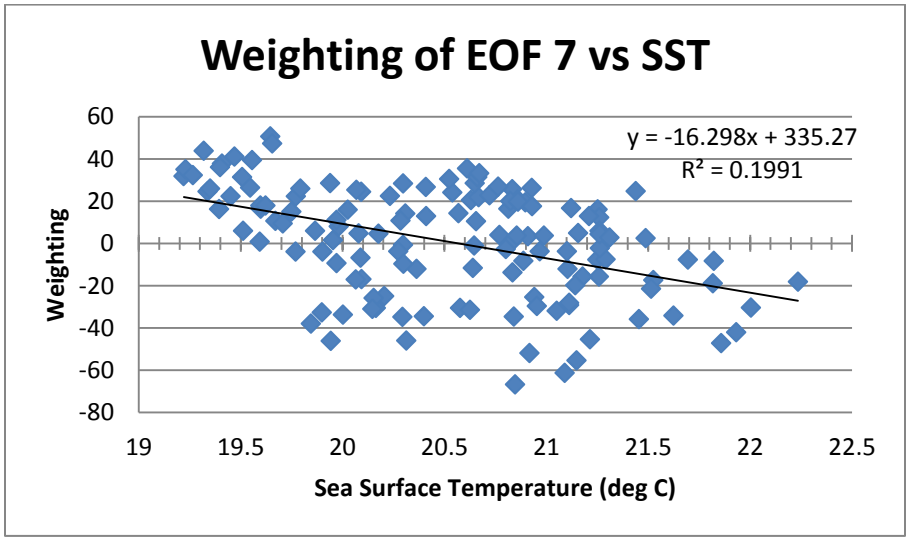

Figure 10: Weighting 7 vs. SST for each Year

The correlation coefficients (R) of weightings on EOF 3 and 7 against SST are 0.4915 and 0.4462 respectively. Therefore, SST and EOF3 as well as SST and EOF7 possess linear relationships considered significant to 95% based on a critical value of 0.1767 (which was determined from interpolating between 100 and 200 to compute the value based on 134 degrees of freedom). Not only do the values surpass the 95% level of significance, but both are significant with 99.9% certainty. Due to the relationship between there variables, the expected values used in the Chi Squared testing need to be recalculated and their significance reevaluated based on those values. It should be noted that the x and y axis of the regression was done with the opposite orientation of the contingency table, therefore the trend is converted to the opposite of what is seen in Figures 9 and 10.

Next the weightings of EOF3 and EOF7 are plotted against each other for the corresponding years. EOFs 3 and 7 are not related with any level of significance based on a correlation coefficient of R = 0.0006, which confirms the expected orthogonality. The test for significance of the Chi Squared values for the storm tables between EOF3 and 7 are valid.

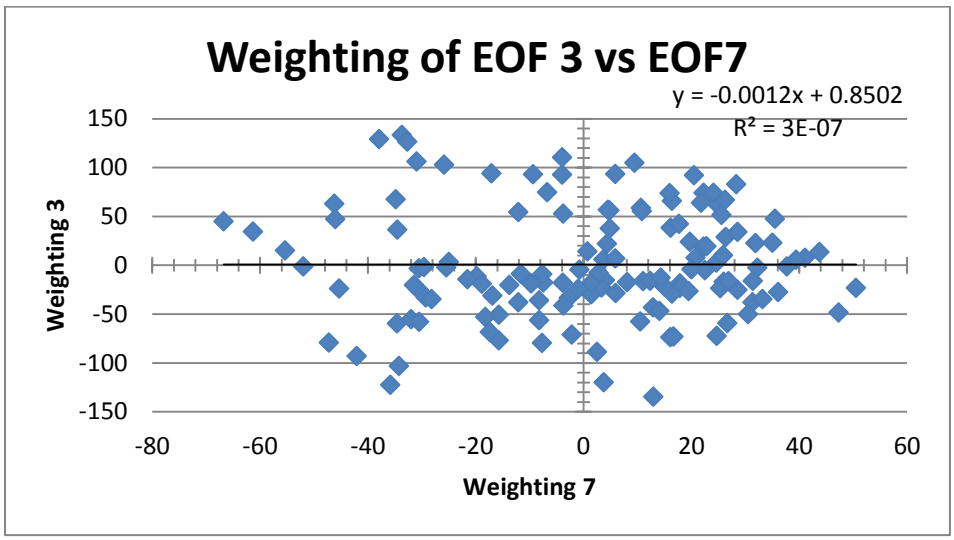

Figure 11: Weighting of EOF3 vs Weighting of EOF7

5.5 REEVALUATING CONTINGENCY TABLES INCLUDING THE EFFECTS OF CORRELATION BETWEEN SST AND EOFs

The relationship between EOF3 and SST as well as the relationship between EOF7 and SST shift the expected values in the contingency tables to higher probabilities following the linear relationship in the bottom left and top right (negative weighting, high SST and positive weighting, low SST). Therefore the expected value will rise in these two regions and fall in the other two. The revised expected values for EOF7 and EOF3 are based on the cumulative probability of the area in each box found by integrating

$$F(w,SST) = \int_{x}^{\infty}\int_{SSTbar}^{\infty} \frac{1}{\sqrt{2\pi}\sigma_{SST}} \exp\left(-\frac{(SST-\overline{SST})^2}{2\sigma_{SST}^2}\right) * \frac{1}{\sqrt{2\pi}\sigma_{res}} \exp\left(-\frac{(w-w(SST))^2}{2\sigma_{res}^2}\right) dSSTdw \ldots\ldots$$

……....Equation 30

Where SST(w) is based on the linear regression:

$w_3(SST) = -38.714SST + 795.05$ ……Equation 31

$w_7(SST) = -16.298SST + 335.27$……Equation 32

With squared correlation coefficients of ρ_3^2=0.4416 and ρ_7^2=0.1991. The residual standard deviation based on correlation and the standard deviation of the weighting is:

$\sigma_{res} = \sigma_w\sqrt{1-\rho^2}$……Equation 33

The standard deviation are: σ_{w3}=55.32271, σ_{w7}=25.65545, σ_{SST} =0.702417 and the mean of SST is 20.51473 degrees Celsius. The integrals are evaluated for the numbers within each category of the contingency table. Based on this integration the expected percentages of the contingency table of EOF3 and SST as well as EOF7 and SST are presented in Tables 16 and 17 below.

Table 16: Expected Probabilities within the Contingency Table for EOF3 and SST

EOF3	$w \leq w_{bar}$	$w > w_{bar}$
$SST \leq SST_{bar}$	0.1682	0.3318
$SST > SST_{bar}$	0.3318	0.1682

Table 17: Expected Probabilities within the Contingency Table for EOF7 and SST

EOF7	$w \leq w_{bar}$	$w > w_{bar}$
$SST \leq SST_{bar}$	0.1765	0.3235
$SST > SST_{bar}$	0.3235	0.1765

Each of these percentages is multiplied by the total number of storms used within the table to compute the expected frequency.

$$Expected = F(w, SST) * total\ storms$$……..Equation 34

The revised contingency tables with respected Chi Squared values based on these alternate probabilities are displayed in Tables 18 and 19.

Table 18: Contingency Table of SST and EOF3 with Revised X^2 Based on Linear Relationship				
Weighting of EIG 3	All Storms		Intense Storms	
	X^2	5.958359	X^2	8.72912
	$w \leq x$	$w > x$	$w \leq x$	$w > x$
$SST \leq SST_{bar}$	8	9	1	0
$SST > SST_{bar}$	20	4	7	4

Table 19: Contingency Table of SST and EOF7 with Revised X^2 Based on Linear Relationship				
Weighting of EIG 7	All Storms		Intense Storms	
	X^2	7.590399	X^2	14.48966
	$w \leq x$	$w > x$	$w \leq x$	$w > x$
$SST \leq SST_{bar}$	6	11	0	1
$SST > SST_{bar}$	21	3	10	1

Given that Tables 18 and 19 have removed the influence of the correlation between SST and each of the EOFs' weightings, the remaining influence of including SST is significant. Although the zero's in the table still compromise the statistical evidence for the intense storms, there it is clear that EOF's 3 and 7 both individually pair with the SST to make favorable conditions for TC to enter the BAV as well as remain intense while the SST is above average and the weightings are below average with a 99% certainty in comparison to a critical value of 6.63.

5.6 TESTING A RELATIONSHIP BETWEEN STORM HEADING AND WEIGHTING

As with previous contingency tables, Table 12 contains two tables, one for all storms and another for only intense storms to determine if the EOF affects storm heading (the storm's path direction in degrees from the horizontal) and again to determine if the EOF has a stronger effect on storm heading for more intense TCs. If there is a relationship between storm heading and weighting, it is likely that more of the storms will be along one of the diagonals of the table. This relationship would show that the large-scale, atmospheric steering currents have an effect over the heading as well as the influence of storm frequencies previously shown. This test is conducted for all of the EOF's, but only tables which display statistical significance in both of the tests (all storms and intense storms) are presented here in Table 20. EOF6 has statistically significant Chi-Squared values both above the 99% certainty critical value.

Table 20: Contingency Table of Storm Angle and Weighting of EOF6

Weighting of EIG 6	All Storms		Intense Storms	
	X^2	6.71	X^2	6.67
	$w \leq x$	$w > x$	$w \leq x$	$w > x$
Angle ≤ 65	8	16	0	4
Angle > 65	12	5	6	2

Previously it was found that EOF6 does not does not affect storm frequency, however, as shown in Table 20, it appears to have a possibly significant effect on the storms' heading. While the weighting of EOF(6) is negative, storms tend to follow higher heading angles paths, and while it is positive storms tend to follow lower heading angles. Although the statistical significance test for intense storms is reduced by a zero in the table, this does show that there is a much higher prominence of storms heading influence by EOF6 while storms are higher intensity.

5.7 DISCUSSION OF THE RELATIONSHIP OF CLIMATE AND TROPICAL CYCLONES

It is clear from many previous studies that large scale circulation plays an important role in the steering of TC's (Xie 2005; Wang et al 2011). Similar to large scale features, semi-permanent, synoptic scale features, tend to control airflow in regions which they inhabit. For example, air flow near a region of high pressure is directed in an outward spiral because air flows from high towards low pressure. These features can also steer other synoptic scale systems (TC's etc.) away from the high. When an area contains a low pressure region, the airflow is directed into the area and around by the Coriolis Effect. This can cause tropical cyclones to be pushed around it and slightly into it with a clockwise direction.

The EOF's describe semi-permanent pressure features of the large scale circulation within this thesis' study region in a reduced number of dimensions. Weightings on these EOF's depend on the similarity of a given pressure field in time to these functions. Thus, the weightings represent the deviations from the mean overall pressure field and can be positive or negative. For example, the pattern shown in Figure 13 with a negative weighting would produce larger than average pressures in the area southeast of Nova Scotia, while a positive weighting would produce lower than normal pressures in this region that are larger with higher magnitude weightings. Therefore the weightings of each EOF can be used effectively to represent the atmospheric state and make a good tool for analysis.

Analyzing storm frequency and intensity for each EOF's weightings provides useful information for quantifying how atmospheric pressure patterns influence storm behavior and is used here as an objective means to identify specific atmospheric pressure patterns affecting the steering currents of synoptic scale features. It is hypothesized that a pressure deviation off the east coast

of the U.S. would be present in the EOF's which affect storm frequency for the BAV because the associated steering would be toward this region. EOF(3) and EOF(7) presented in Figures 12 and 13 are both found to relate with storm frequencies in the BAV and will be discussed in the paragraphs below as to why they may be affecting storm frequency.

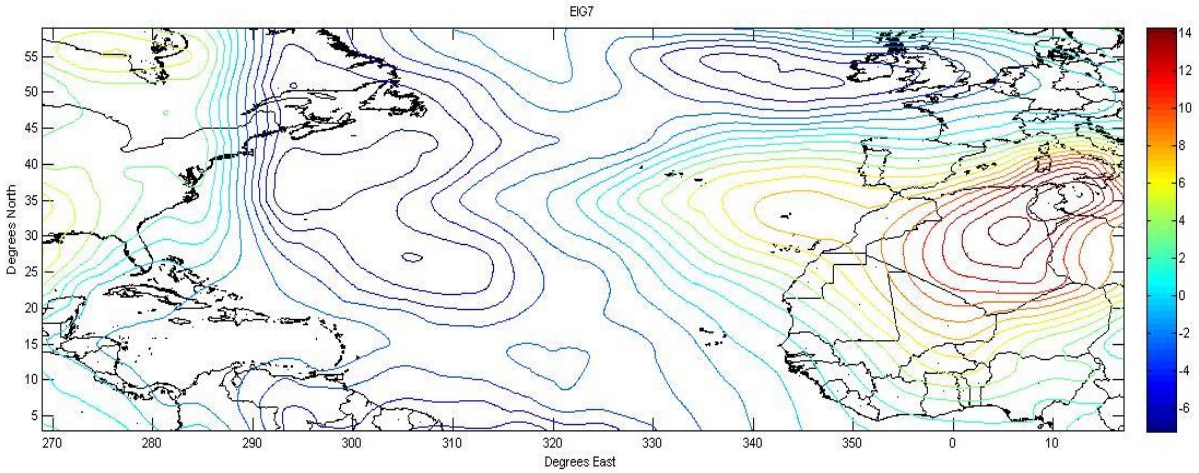

Figure 12: Contours of EOF(7) Showing Semi-Permanent Circulation Aspects

In general, the major storm events in the BAV occurred while there was a negative weighting on EOF(7). This state is associated with higher than average pressures over the Atlantic Ocean off the northeast coast of North America. Counterclockwise flow around this high-pressure, large-scale system would tend to steer storms toward United States coastal areas. If a storm is traveling north along the Atlantic Coast of the US, this region of higher pressure would tend to steer it toward the New York region. The statistical significance of the relationship between storms entering the BAV and negative weightings on EOF(7) supports the existence of important impacts on storm frequency produced by the atmosphere. This is more apparent during intense storms which have larger potential coastal impacts.

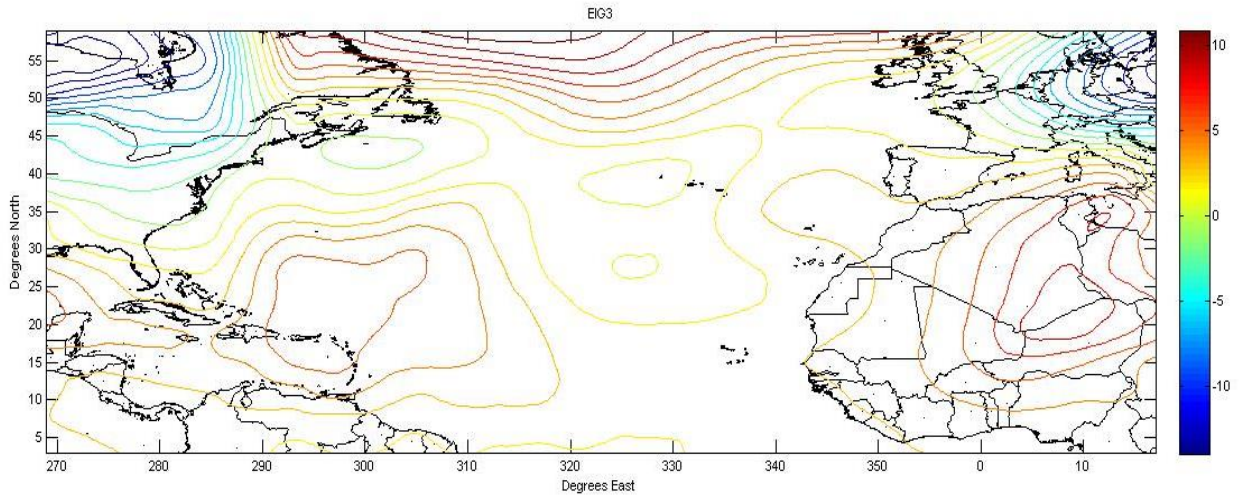

Figure 13: Contours of EOF 3 Showing Semi-Permanent Circulation Aspects

Local pressure perturbations of EOF(3) in the region off the northeast U.S. coast are similar to those of EOF(7), therefore it is also likely this pressure field would have a similar effect over TCs during times of a negative weighting. While a negative weighing exists for EOF(3), there is a high pressure region just off the Nova Scotia and Maine as well as a high covering a large majority of the eastern U.S. This atmospheric pattern would tend to influence storms into the BAV because there is a space between the two highs directly over the New York area. The relationship between storm probability and the negative weighting is consistent with the statistically significant relationship found between the weighting of EOF(3) and storm frequency and intensity.

Figure 14 shows the sea surface pressure during the 1938 storm. The yellow line shows the tropical cyclone's predicted path, and the green shows its actual path. The storm was forced into the New York area by the combined effects of the high pressure systems to either side. Based on the statistically significant relationships between EOF(3) and EOF(7) and storm frequency and

intensity, it is probable that many of the other storms which came into the BAV occurred while sea surface pressure was similar to that shown in Figure 14 which depicts similar features to those of EOF(3) and EOF(7).

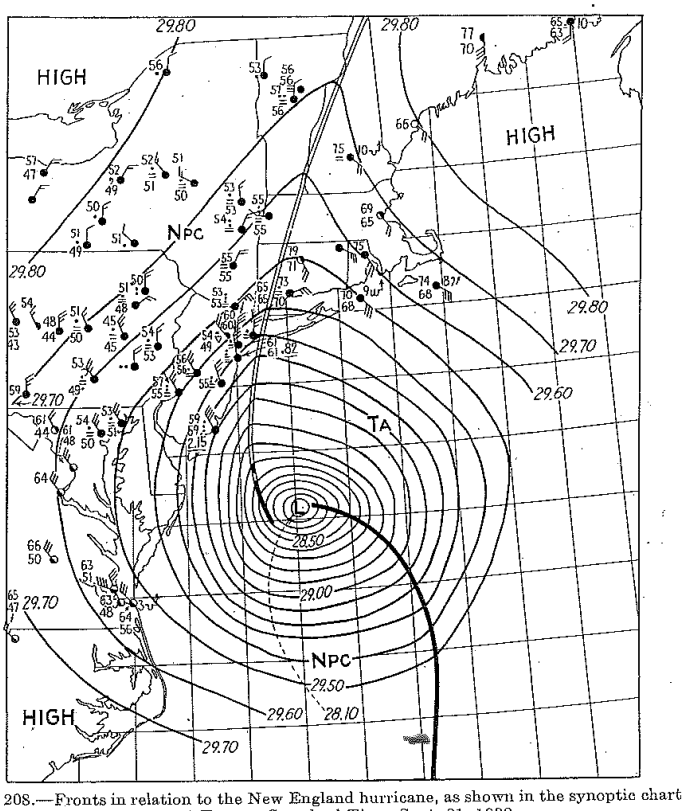

FIG. 208.—Fronts in relation to the New England hurricane, as shown in the synoptic chart for 1200 Eastern Standard Time, Sept. 21, 1938.

Figure 14: 1938 Storm Track and Sea Surface Pressure (Byers 1944)

While EOF(7) and EOF(3) drive storms into the region, the storms are being directed further along a more specific path by EOF(6) (Figure 15). This pressure variation is significantly affecting the direction which storms follow and should be considered within hazard probabilities because it would greatly affect surges in the region due to the large dependence of setup on angle

of incidence for land-falling storms (Irish and Resio 2010). This relationship presents another aspect of the natural influence of large scale circulation on storm behavior for the BAV that should be used within hazard probabilities.

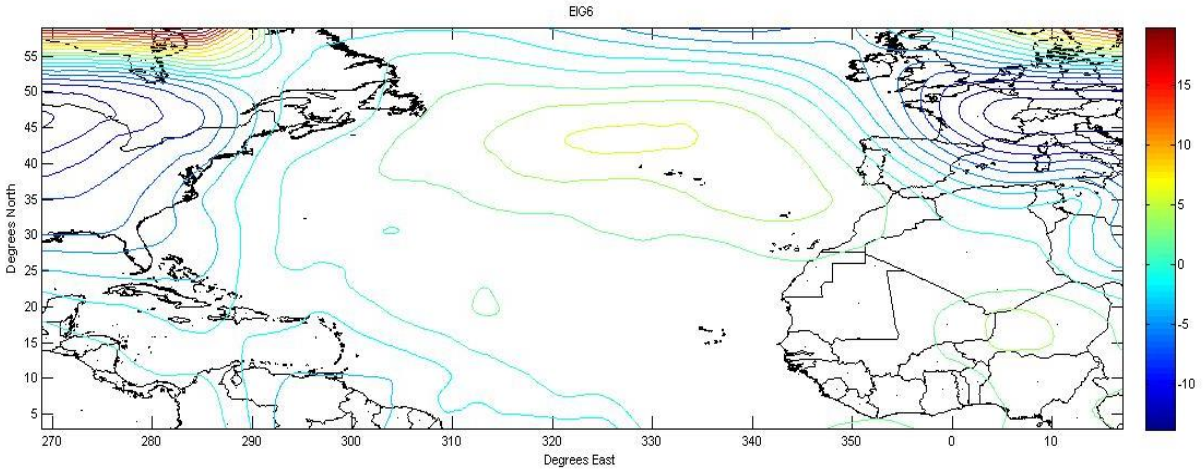

Figure 15: Contours of EOF(6) Showing Semi-Permanent Circulation Aspects

Also in this thesis, sea surface temperature variations, represented by a five-year time centered average, are investigated because SST is known to be a factor in storm intensity and is used to calculate maximum potential intensity (MPI) (Holland 1997; Emanuel 1997). Tropical cyclones acquire their fuel from the latent heat of the ocean surface, therefore higher temperatures, induce higher intensity storms. Only one out of the twelve intense storms (Storms with Cp below 980mb) occurred when the temperature was below average (20.5˚C), and that SST was not close to the lowest it has been in recorded history for this region. Figure 16 displays the time centered sea surface temperature at the Battery tide gauge. During many of the years with the major storms in the region, the SST's were at local maximum temperatures. Since 1995, the sea surface temperature at the BAV has not fallen below 21˚C which coincides with the beginning of the period which NOAA declared there would be heightened storm activity for the Atlantic Coast

of the U.S (Goldenberg et al 2001). The SST for this region combines with EOF(3) and EOF(7) to drive intense tropical cyclones into the BAV supported by a statistically significant relationship.

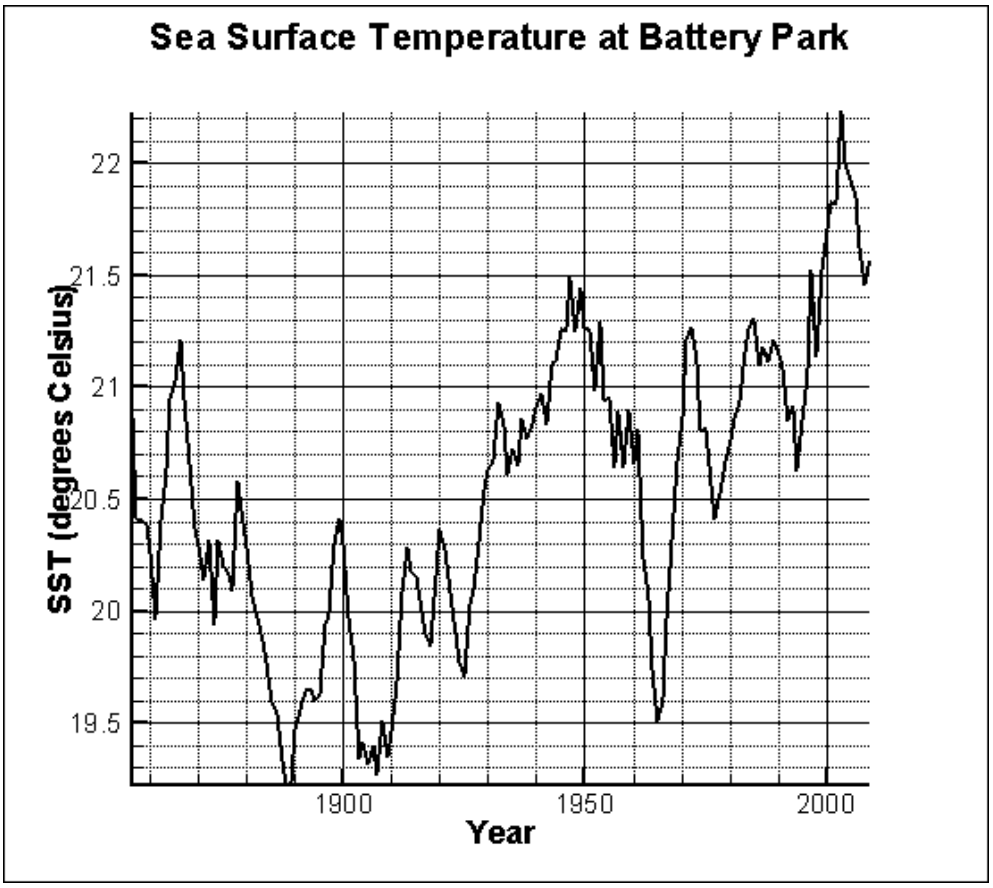

Figure 16: Seasonal, Time-Centered, Five-Year Average SST at Battery Park

The significant relationships with storm probability of EOF(3) and EOF(7) for the BAV can assist with storm probability estimation and EOF(6) for storm angle probability estimation for the BAV. The Poisson frequency estimation and omnidirectional probability are leading to misestimation in storm probabilities which can be improved using variable hazards based on atmospheric and oceanic influences characterized by the weightings on EOF(3), EOF(7) and EOF(6) and SST. Because SST and the weightings of EOF(3) and EOF(7) are related, it is likely

that the climate works in various ways (potentially caused by one another) determining the intensity and paths which storms can take during a given period which can be quantified into hazards. The atmosphere does not behave independently and neither should the probabilities of natural phenomenon within it.

CHAPTER 6 RESULTS OF PART 2: EVALUATION OF PARAMETER RELATIONSHIPS RELATIVE TO HAZARD ESTIMATES

6.1 STORM INTENSITY VS. ANGLE

The dataset used here cuts off many of the storms exhibiting low heading angles (almost all below 45˚) because of the 45˚ angle which the storms must pass into to be included in this study. A histogram is made to illustrate the heading angles which the storm tracks follow, as shown in Figure 17.

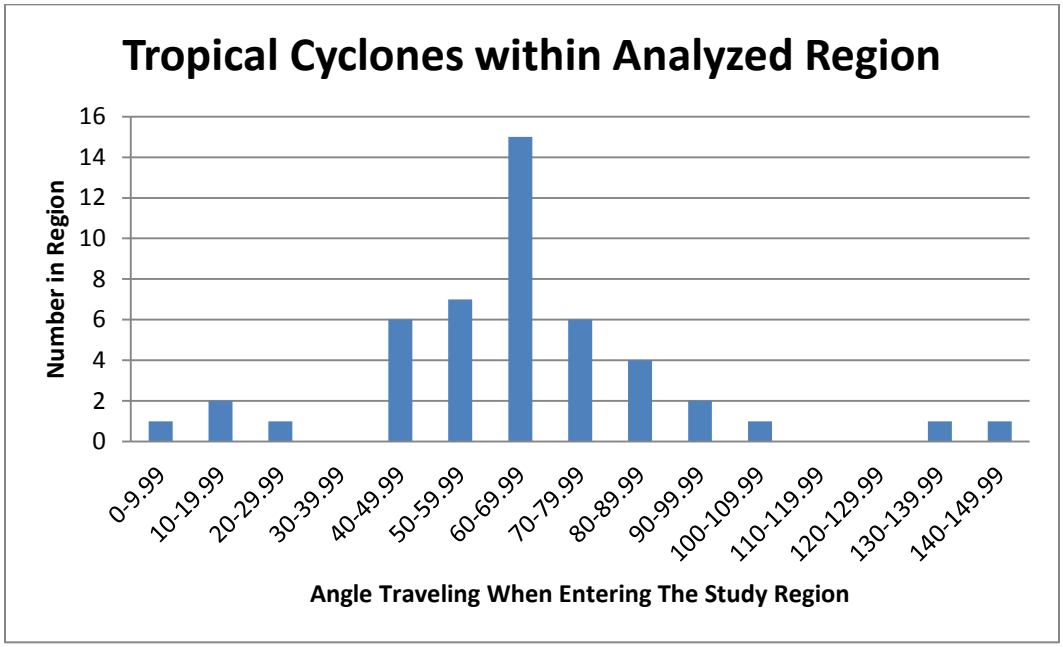

Figure 17: Histogram of Storm Angles

Hazard calculations for this area are estimated using a normal distribution with mean direction of 22 degrees east from north and 10 degree standard deviation (or 68 degrees from the horizontal, which is the system used here) (FEMA 2012). According to these assumptions for the storm heading, 99% of the storms should be within three standard deviations, therefore between 38 and 98 degrees. There are 47 storms used within this set, therefore less than 1 of these storms should

be out of this region, yet 7 storms are outside of three standard deviations, as illustrated in Figure 17.

After sorting the storms based on angle, it was found that about 50% of the storms within the study region were below 65 degrees and about 50% were above; it was not a perfect split, but to split at a whole number it was the best option; 15 storms fell below this value and 13 fell above. This set is limited to 28 storms because the minimum central pressure values were not available for all of the storms, especially in the earlier years. The average Cp for each of the sets is displayed in Table 21.

Table 21: Central Pressure Statistics by Direction

Angles < 65 degrees		Angles > 65 Degrees	
Average Cp	990.867	Average Cp	972.2308
S(Cp)	16.2343	S(Cp)	20.33123
n	15	N	13

The average of the minimum Cp of the storms is lower (more intense) for the storms which traveled with higher heading angles. The values are separated by about 18 mb, which is substantial considering the consequences of the two different storm intensities. These means are tested for a significant difference through the Student's t test resulting with a t value of 2.70 to be compared to a critical t value of 2.056 for a two-tailed t test based on 26 degrees of freedom and a 95% certainty. Because the calculated t is higher than the critical value, the null hypothesis that the means are equal is rejected therefore concluding that there is a difference between the sets. This finding implies an inter-connectivity between storm heading and intensity therefore

the two parameters are plotted against each other in Figure 18. The data appears to follow a linear with a regression formed where

$$Angle = -0.549Cp + 607.68 \quad \text{.....Equation 35}$$

with a correlation coefficient of R=0.5 which is must be above the value, 0.42, to be considered significant for 26 degrees of freedom. Therefore, with statistical significance with 95% certainty, there is a relationship between higher heading angles and higher intensity of storms. This information would lead to a difference in the hazard assessment for the region because the estimated joint probability is considered to be independent. Higher heading angles for this area result in higher surges because of the set up this coastal geometry causes, so if the higher angles are also higher intensity, the surge risk would rise significantly.

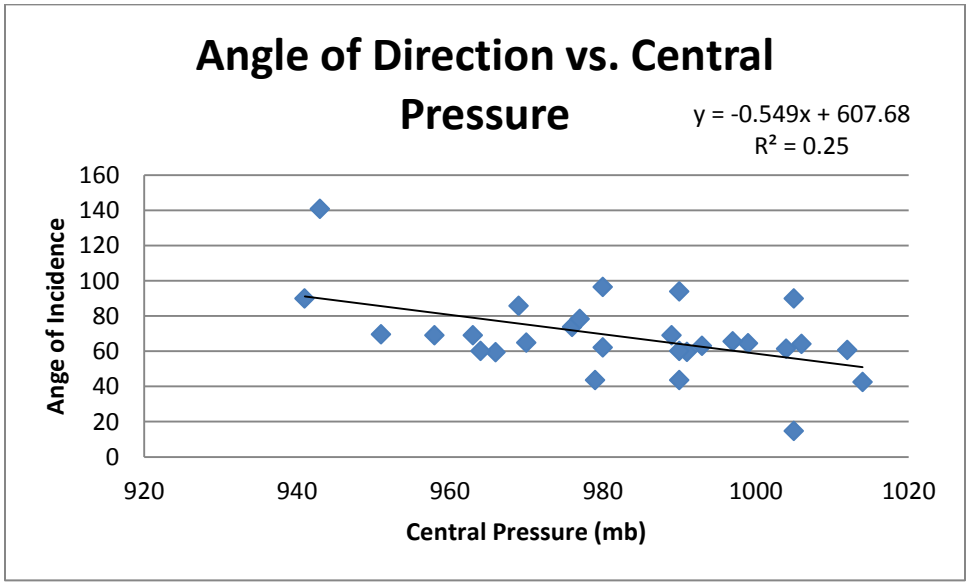

Figure 18: Angle of Direction vs. Central Pressure

To quantify the influence of this difference in risk, a Gumbel ranking (Figure 19), is plotted for the three different datasets: one with heading above 65 degrees, one with heading below 65 degrees, and one with both sets included into one. Each of the regressions trend with different

slopes, and although it is hard to visualize in a log scale, the graph shows a difference in trend between the sets, causing an exponential difference for higher return periods. This suggests that analyses done assuming one population of storms without separating by angles traveled, causes an underestimation in intensity hazard and a resulting inability to properly mitigate.

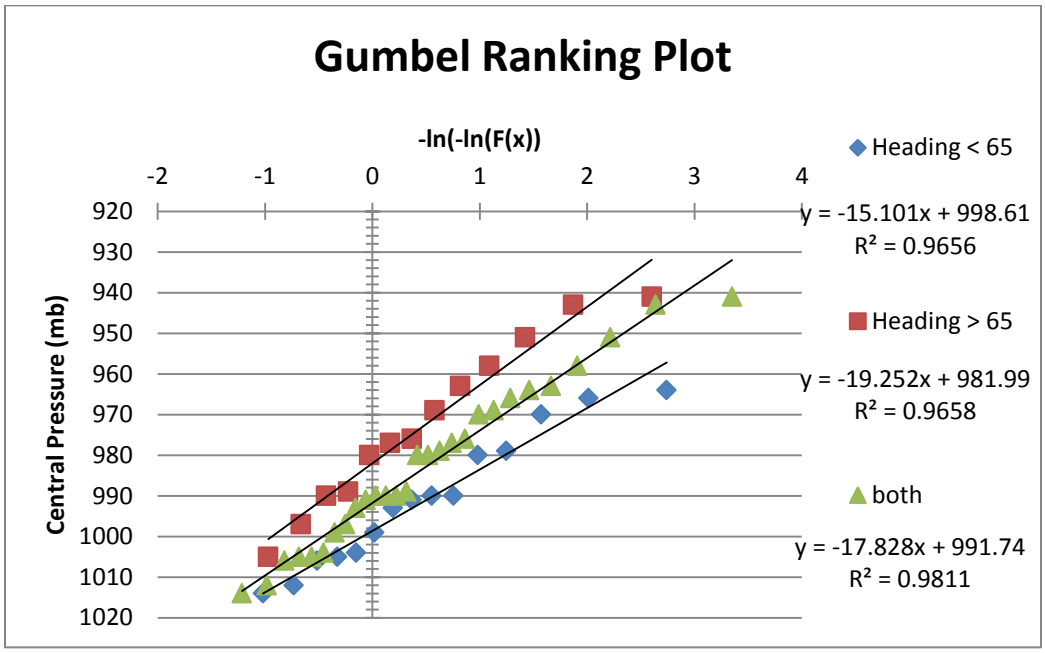

Figure 19: Gumbel Ranking for Central Pressures Differentiated by Angles

A plot of the return periods for each of the three sets (above 65, below 65, and the set consisting of all the storms) in Figure 20 is based on the Gumbel ranking regression (Figure 19).

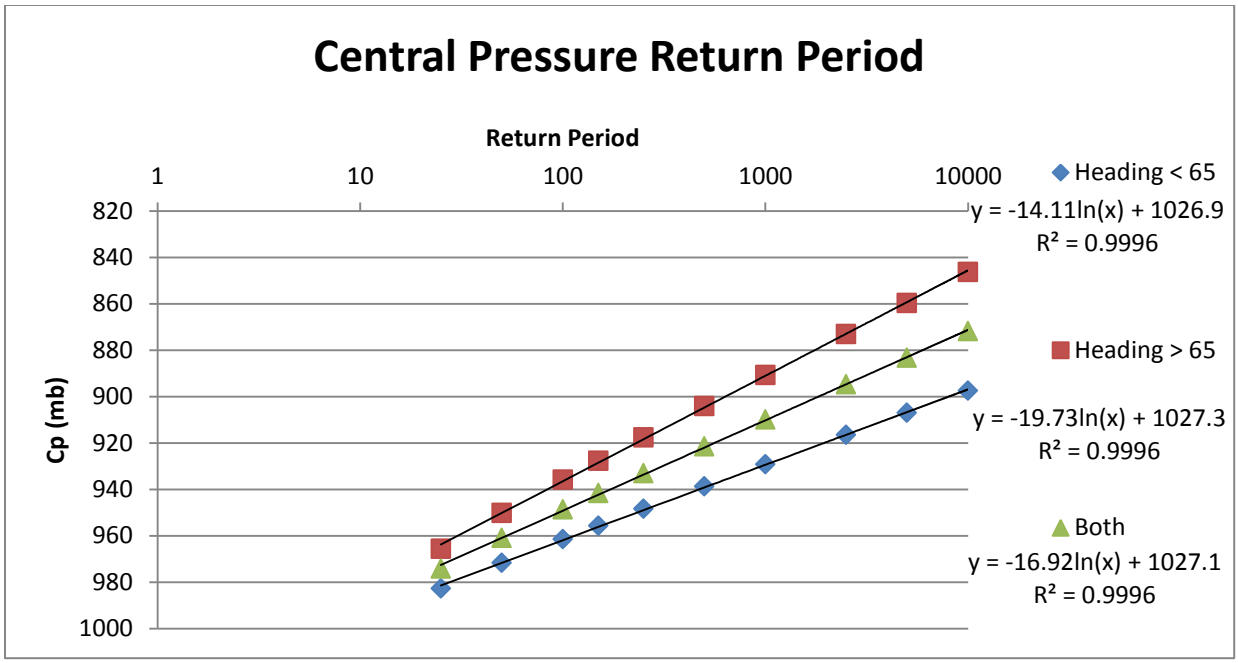

Figure 20: Return Period of Central Pressure based on Storm Angle

The values of return period are significantly different for the three different datasets. For the high angle return, this graph suggests a 70 year return period, while the low angle suggests a return period of 380 years for a storm of Sandy's intensity. This return period represents storm angle, intensity and Poisson frequency, which are the most significant factors in determining storm surge hazard. Thus, these results suggest that not separating storm by angle causes an underestimation in storm surge return periods and will result in an inability to properly mitigate the risks associated.

6.2 RELATIONSHIP BETWEEN CENTRAL PRESSURE AND FORWARD VELOCITY

Within the FEMA calculations of hazard, the forward velocity is a function of the pressure differential (peripheral pressure – central pressure) with a linear relationship; here, this relationship is tested (FEMA 2012). Here central pressure instead of the difference in pressure assuming that the outside pressure is similar for each of the storms which is assumed to be 1012

through FEMA's analysis (FEMA 2012). A plot of Cp verse Vf was formed and displays no linear relationship visually as well as no statistically significant relationship present (Figure 21).

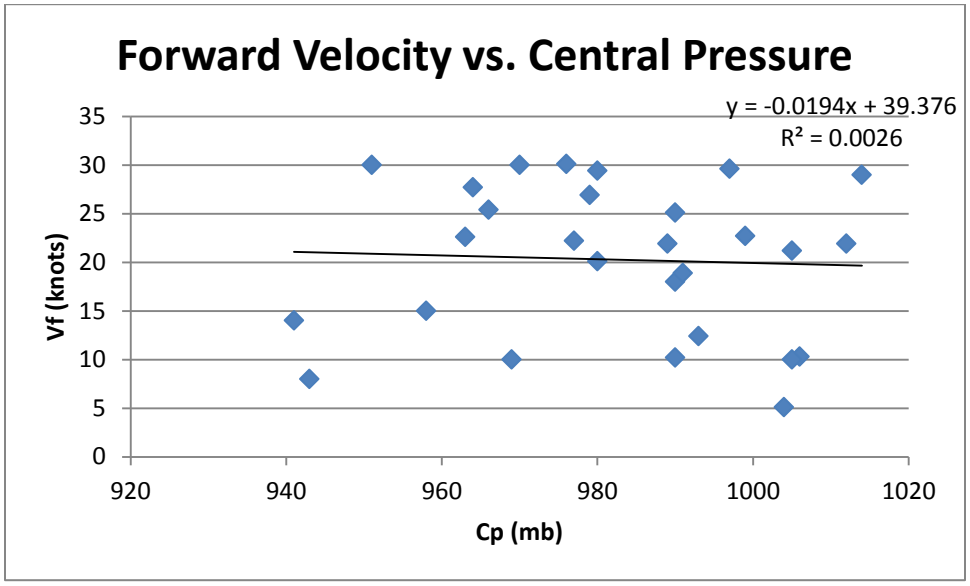

Figure 21: Forward Velocity vs. Surface Pressure Regression

Although this dataset is not a random sample of the storms in the region, it should generally follow the relationship presented or show some form of correlation between the two parameters if a relationship does exist. The objective criteria used here for storm selection was done to represent the storms presumed to have the most detrimental impact on the BAV. This lack in relationship between hazardous storms' forward velocity and central pressure suggests that the probabilities should not be calculated using this dependence.

6.3 HAZARDOUS STORM DISTRIBUTION

The frequency of the time in years between all storms is compared to a theoretical exponential distribution based on the Poisson frequency to test the validity of the assumption that TCs follow a Poisson distribution. A graph of the observed frequency is overlaid by the theoretical, exponential frequency is shown in Figure 22.

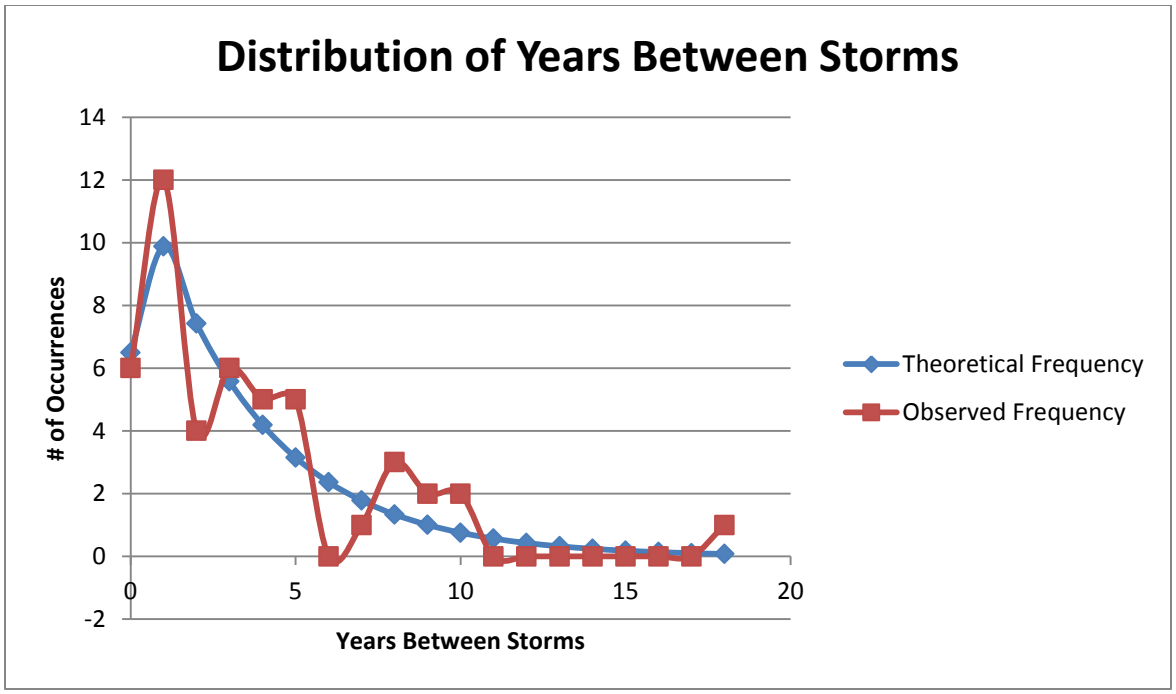

Figure 22: Frequency of Time Between All Observed Storms Compared to Theoretical Poisson

There appears to be a relative consistency between the two distributions which is tested for significance using the Chi Squared test statistic. The contingency table was separated into four year intervals to eliminate a large number of zero's which can control the results. Chi Squared is shown in the Table 22 to be 4.38, which is not a high enough value to reject the null hypothesis that the two values are equal based on four degrees of freedom and a 95% certainty (critical value=7.81) suggesting that the frequency follows this relationship, but not with statistical significance.

Table 22: Contingency Table of Frequency of All Storms Observed Compared to Theoretical Exponential Frequency					
	0-3 Y	4-7 Y	8-11 Y	12-15 Y	16-19 Y
Observed	28	11	7	0	1
Theoretical	26.47885	13.29573	4.240095	1.352194	0.431224
((O-E)^2)/E	0.087387	0.396395	1.79644	1.352194	0.750206
X^2			4.382622819		

To determine if the intense storms behave with a different assumed return period, they are tested using a separate distribution based on only the number of intense storms in this time period. The observed frequency and theoretical frequency are shown in Figure 23. These two appear to be less similar than the time occurrence between all storms distribution and its theoretical exponential distribution.

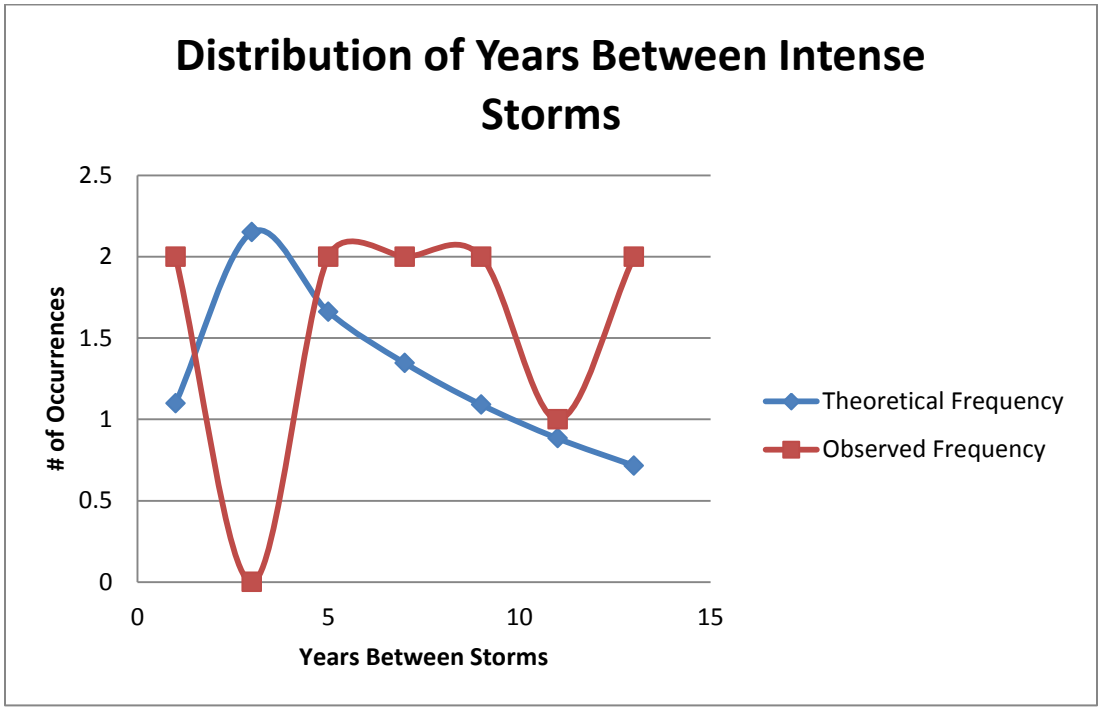

Figure 23: Observed Frequency of Time Between Intense Storms Compared to Theoretical Poisson Frequency

The contingency table of these two distributions is shown in Table 23. For this case, we also do not reject the null hypothesis that the two sets are not equal. Although it visually appears that the two distributions differ significantly, there is not enough statistical evidence to support this statement.

Table 23: Contingency Table of PDF of Intense Storms Compared to Theoretical Exponential Distribution

Years Bet Events	0-1 Y	2-3 Y	4-5 Y	6-7 Y	8-9 Y	10-11 y	12-13 Y
Observed	2	0	2	2	2	1	2
Theoretical	1.099036111	2.150408	1.661225	1.345854	1.090354	0.883359	0.71566
((O-E)^2)/E	0.738588951	2.150408	0.069087	0.317944	0.758886	0.015402	2.304905
	X^2			6.355220831			

6.4 PROBABILITIES OF SANDY AND IRENE

As discussed in the introduction, Hurricanes/ Tropical Cyclones Sandy and Irene are associated with extremely low probabilities for some of their parameters when these probabilities are quantified from the assumed distributions found in Table 1 (FEMA 2012). Each of the parameters is quantified as discussed in the methodology section 4.2.3. The associated parameter probabilities are presented in Table 24 where F(x) is the cumulative probability up to parameter associated with each storm, E(x) is the exceedance probability and T(x) is the return period in years.

Table 24: Probabilities of the Individual Parameters of Sandy and Irene

Parameter	Irene			Sandy		
	F(x)	E(x)	T(x)	F(x)	E(x)	T(x)
θ	0.4043	0.5957	1.6787762	0.9998	0.00015	6578.9474
Rp	0.8044	0.1956	5.1124744	0.9948	0.00523	191.02197
vf	0.9541	0.0459	21.805257	0.9998	0.0002	5089.0585
Δp	0.6236	0.3764	2.6567481	0.8745	0.1255	7.9681275

A joint probability for the parameters can be calculated using a computer model, but inferring the probabilities observing that Irene is not an uncommon storm, but to occur the year before a storm with parameters similar to Sandy is extremely improbable and may be considered seemingly impossible.

6.5 DISCUSSION OF CURRENT HAZARD ESTIMATES FOR TROPICAL CYCLONES

Current hazard estimates include a large amount of bypassing storms which pose no major threat to the BAV, therefore should be excluded from the storm population used to estimate surge hazards. Conventional hazards are calculated to prepare for the expected surge within a given 100 year period. This calculation of previous storm probabilities appears to be biased because of the inclusion of a large population of storms that did not threaten NYC which caused the distributions and relationships to be misrepresented in this region. The storms within the objective dataset here based on the most hazardous impact to the BAV, appear to behave in a different manner than the bypassing storms. Filtering the dataset shows relationships which exist in the land-falling, intense storms that were previously neglected and allows for more accurate probability calculations based on the storms which do pose a major threat, in turn allowing for proper mitigation.

As a whole, TC occurrences appear to follow a Poisson distribution based on statistical analysis which is further supported by the visual representation of the data. However, the intense storms do not appear visually to mimic this distribution, but there is not enough statistical evidence to claim otherwise. Based on the findings here, it is hypothesized that this lack in statistical evidence is due to epistemic uncertainty caused by a lack in data. If the sample followed the same pattern, but had double the amount of storms, the contingency table would change dramatically as shown in Table 25.

Table 25: Contingency Table of Intense Storms' Distribution if the Data were Doubled

Years Bet Events	0-1 Y	2-3 Y	4-5 Y	6-7 Y	8-9 Y	10-11 y	12-13 Y
Observed	4	0	4	4	4	2	4
Theoretical	2.198072222	4.300817	3.322451	2.691709	2.180709	1.766718	1.43132
((O-E)^2)/E	1.477177903	4.300817	0.138173	0.635888	1.517773	0.030803	4.60981
	X^2			12.71044166			

This table would represent enough statistical evidence to reject null hypothesis that the two distributions are not equal. Based on the data currently possessed for the BAV of intense storms, these storms may follow a Poisson distribution, but need to continue to be investigated as more data is accumulated because if they continue on this trend, it will be clear that storms do not follow this assumed distribution.

CHAPTER 7 CONCLUSION

Atmospheric circulation is affecting storm behavior in the New York region, as shown here by the statistically significant relationship found between storm frequency and intensity in the BAV that exists for both atmospheric states characterized by a negative weighting on EOF's 3 and 7. These relationships increase in significance while coupling with sea surface temperatures that are related to these circulation patterns. EOF6 also possesses a statistically significant relationship with the heading tropical cyclones are directed in upon entering the New York region. These relationships were determined using objective representations of surface pressure to analyze their influence and display a significant variability of storm behavior dependent on the climate. Proper mitigation is dependent upon using this variability to quantify a more accurate probability of storms entering the BAV, otherwise the hazard estimates will continue to underestimate hazard causing a lack of preparedness and resilience for the largest city in the United States.

This thesis shows that a common assumption in hazard quantification (that storms are constant through time following a Poisson distribution) may be inaccurate for more intense storms and needs to be continually investigated. There is an underlying interconnectivity in nature which is greatly affecting storm hazards for the New York City area. There is a statistically significant relationship between TC heading and intensity for the BAV which is currently being neglected in hazard estimates causing an underestimation in probabilities. Heading and intensity coupling together causes a significant rise in storm damages because the associated surges are greatly dependent on these characteristics: angle of incidence and central pressure. This underlying

relationship between storm direction and intensity appears to be the result of the dependence of storms behavior on large scale climactic variations and is influencing the hazard probabilities.

Atmospheric circulation affects 1) the oceanic currents, along with local heating and cooling of the surface water layer, and 2) the atmospheric steering for tropical cyclones. Heightened sea surface temperatures result in more available latent heat for tropical cyclones causing their intensity to increase. As shown here, stronger cyclones are more likely to travel with an angle much closer to shore normal which significantly increases the potential surge hazard, drastically increasing the damages to the BAV. This natural behavior brings up nuances which are often neglected while quantifying hazard for this region. Storms within the BAV do not appear to be the sum of random coincidences, but instead a result of coupled processes of many scales in nature.

To properly quantify and mitigate hazards in this region, the natural coupling must be included while determining the probabilities as well as properly filtering the data used for hazardous storms. For example, the calculation of parameter distributions and the relationships they follow should exclude storms that do not pose a threat to the area in question otherwise the bypassing storms will unduly influence these estimates, causing inaccurate relationships and underestimated hazard probabilities. The more comprehensive perspective on hazards adopted here should more accurately represent storm hazard for the BAV and will be revisited in future work.

REFERENCES

(Byers 1944)
Byers, H. R., "General Meteorology" McGraw Hill Book Company, New York and London (1944)

(Cameron 2012)
Cameron, C., "NYC Public Transit Remains Shuttered after Hurricane Sandy Wreaks Havoc on Entire System" (2012). Retrieved from: http://inhabitat.com/nyc/nyc-public-transit-remains-shuttered-after-hurricane-sandy-wreaks-havoc-on-entire-system/

(Dougherty 2001)
Dougherty, C., "Statistical Tables" (2001). Retrieved from: http://course.shufe.edu.cn/jpkc/jrjlx/ref/StaTable.pdf

(Emanuel 1987)
Emanuel, K., "The Dependence of Hurricane Intensity on Climate," Nature Volume 326, No. 6112, pp. 483-485. Retrieved from: ftp://texmex.mit.edu/pub/emanuel/PAPERS/nature87.pdf

(Emanuel 1988)
Emanuel, K., "The Maximum Potential Intensity of Hurricanes. J. Atmos. Sci, 45, 1143-1155. (1988)

(Emanuel 2007)
Emanuel, K., "Environmental Factors Affecting Tropical Cyclone Power Dissipation," Journal of Climate (November, 2007) pp. 5497-5509. Retrieved from: ftp://texmex.mit.edu/pub/emanuel/PAPERS/Factors.pdf

(FEMA 2012)
Toro, G. Operating Guidance No. 8-12 for use by FEMA Staff and Flood Hazard Mapping Parameters. (March 2012)

(Goldenberg 2001)
Goldenberg, S. B., Landsea, C., Mestas-Nunez, A. M., and Gray, W. M., "The Recent Increase in Atlantic Hurricane Activity," Science 293, doi:10.1126/science.1060040, (2001), pp. 474-479.

(Gray 1984)
Gray, W. M., "Atlantic Seasonal Hurricane Frequency. Part 1: El Nino and 30mb Quasi-Biennial Oscillation Influences," Monthly Weather Review Volume 112 (September, 1984), pp. 1649-1668. Retrieved from: http://hurricane.atmos.colostate.edu/Includes/Documents/Publications/gray1984-1.pdf

(Holland 1997)
Holland, Greg J., "The Maximum Potential Intensity of Tropical Cyclones." J. Atmos. Sci., 54, 2519–2541. (1997) Retrieved From: http://dx.doi.org/10.1175/1520-0469(1997)054<2519:TMPIOT>2.0.CO;2

(HuiJun 2007)
HuiJun, W., JianQi, S., Ke, F., "Relationships Between the North Pacific Oscillation and the Typhoon/ Hurricane Frequencies," Science in China Series D: Earth Series Volume 50 No. 9 (September, 2007), pp. 1409-1416. Retrieved from: http://download.springer.com/static/pdf/242/art%253A10.1007%252Fs11430-007-0097-6.pdf?auth66=1391796876_2ef93fee96a0017a5008f82b0f9f8a2b&ext=.pdf

(HURDAT2 2013)
Landsea, C., Franklin, J., Beven, J., "The Revised Atlantic Hurricane Database: HURDAT2." National Hurricane Center (February 2013). Retrieved from: http://www.aoml.noaa.gov/hrd/hurdat/hurdat2_1851_2012-jun2013.html

(Irish and Resio 2010)
Irish, J. L., and Resio, D. T., "A hydrodynamics-based surge scale for hurricanes", Ocean Eng. [Special Issue, Interagency Performance Evaluation TaskForce (Hurricane Katrina), Z. Demerbilik, (ed.)], 37(1), 69-81, (2010).

(Kossin et al. 2010)
Kossin, J.P., Camargo, S. J., Sitowski, M., "Climate Modulation of North Atlantic Hurricane Tracks," Journal of Climate Volume 23 (June 2010), pp. 3057-3076. Retrieved from: http://www.ssec.wisc.edu/~kossin/articles/Kossin_et_al_2010_JofC.pdf

(Minchillo 2012)
Minchillo, J. Photojournalist (2012). Retrieved from: http://www.johnminchillo.com/#/superstorm-sandy/superstorm01

(NOAA 1987)
Ho, F. P., Su, J. C., Hanevich, K. L., Smith, R. J,, Richards, F.P, Spring, S., "Hurricane Climatology for the Atlantic and Gulf Coasts of the United States," NOAA Technical Report NWS 38, (April, 1987).

(NOAA 2013)
NOAA: Tides and Currents. (2013), Retrieved from: http://tidesandcurrents.noaa.gov/sltrends/sltrends_station.shtml?stnid=8518750

(NOAA NHC 2013)
NOAA, NHC, Atlantic Season Outlook Update: Press Release (August 2013) Retrieved from: http://www.cpc.ncep.noaa.gov/products/outlooks/hurricane.shtml

(NYC 2009)
The City of New York, "Natural Hazard Mitigation Plan"(March 2009) Retrieved From: http://www.nyc.gov/html/oem/downloads/pdf/hazard_mitigation/full_hmp_march_2009.pdf

(PRMSL 2012)
Compo, G.P., J.S. Whitaker, P.D. Sardeshmukh, N. Matsui, R.J. Allan, X. Yin, B.E. Gleason, R.S. Vose, G. Rutledge, P. Bessemoulin, S. Brannimann, M. Brunet, R.I. Crouthamel, A.N. Grant, P.Y. Groisman, P.D. Jones, M. Kruk, A.C. Kruger, G.J. Marshall, M. Maugeri, H.Y. Mok, A. Nordli, T.F. Ross, R.M. Trigo, X.L. Wang, S.D. Woodruff, and S.J. Worley, 2011: "The Twentieth Century Reanalysis Project". Quarterly J. Roy. Meteorol. Soc., 137, 1-28. DOI: 10.1002/qj.776. Retrieved from: http://www.esrl.noaa.gov/psd/cgi-bin/db_search/DBSearch.pl?Dataset=NOAA-CIRES+20th+Century+Reanalysis+Version+2&Variable=Mean+Sea+Level+Pressure

(Resio and Orelup 2007)
Resio, D. T., Orelup, L., "Climatic Variations in Hurricane Characteristics and their Potential Effects on Waves and Surges in the Gulf of Mexico," 9th Waves Workshop (2007). Retrieved from: ftp://ftp.wmo.int/Documents/PublicWeb/amp/mmop/documents/JCOMM-TR/J-TR-34-9th-waves-workshop/Papers/Resio_Orelup.pdf

(Resio et al 1973)
Resio, D. T., Vincent, L., Fisher, J., Hayden, B., Dolan, R.,"Classification of Coastal Environments: Analysis Across the Coast Barrier Island Interfaces" Office of Naval Research, Technical Report No. 5. (February 1973)

(Rodin et al 2013)
Rodin, J. et al, NYS 2100 Commission: Recommendations to Improve the Strength and Resilience of the Empire State's Infrastructure. The Rockefeller Foundation (2013). Retrieved from: http://www.rockefellerfoundation.org/uploads/files/7c012997-176f-4e80-bf9c-b473ae9bbbf3.pdf

(Shay 2000)
Shay, L. K., Goni, G. J., Black, P. G., "Effects of a Warm Oceanic Feature on Hurricane Opal," Monthly Weather Review Volume 128 (February 1999), pp. 1366-1383. Retrieved from: http://www.aoml.noaa.gov/phod/cyclone/data/pubs/Opal.pdf

(Vickery and Wadhera 2008)
Vickery, P.J., Wadhera, D., 2008. Statistical models of Holland pressure profile parameter and radius to maximum winds of hurricanes from flight level pressure and H*Wind data. J. Appl. Meteorol. 47, 2417–2497.

(Wang 2007)
Wang H J, Fan K. "Relationship between the Antarctic oscillation and the western North Pacific typhoon frequency," Chin Science Bull, Volume 52 No. 4, (2007), pp. 561—565

(Wang et al 2011)
Wang, C., Liu, H., Lee, S. K., Atlas, R., "Impact of the Atlantic Warm Pool on United States Landfalling Hurricanes," Geophysical Research Letters Volume 38 L19702, (October 2007). Retrieved from: http://www.aoml.noaa.gov/phod/docs/Wang_etal_2011.pdf

(Wilkinson 1965)
Wilkinson, J.H., "The Algebraic Eigenvector Problem" Oxford: Clarendon Press (1965)

(Xie et al 2005)
Xie, L., Yan, T., Pietrafesa, L. J., Morrison, J. M., Karl, T., "Climatology and Interannual Variability of North Atlantic Hurricane Tracks," Journal of Climate Volume 18 (March 2005), pp. 5370-5381. Retrieved from: http://journals.ametsoc.org/doi/full/10.1175/JCLI3560.1

APPENDIX A

The EOFs were generated by a computer program written by Professor Donald Resio which produces EOFs for a covariance matrix which the user inputs. This system identifies the organization in a multidimensional structure by identifying axes of maximum variance which are orthogonal to all previous axes identified.

The technique utilized here to identify such a coordinate system is called Principal Component Analysis. This technique transforms a covariance matrix, C, by rotating it into diagonal form. The diagonal elements, $\gamma 1 \ldots \gamma n$ are the only non-zero elements. The solution of these elements remains in fundamental algebra which solves for these values through a setoff homogenous linear equations of n unknowns as shown in equation 1.

$Cx = \gamma x$ ……...Equation 1

(C is the covariance matrix, x is a set of orthogonal column vectors (x_1 to x_n) and γ is a diagonal matrix) This equation's solution is done through a nontrivial solution (Wilkinson 1965). Rewriting yields:

$(C - \gamma I)x = 0$ ……Equation 2

(I is the identity matrix) If the determinant is singular this simplification can be made:

$|C - \gamma I| = 0$ ……..…… Equation 3

The eigenvalues are the elements of the diagonal matrix, γ. A set of n column vectors in the matrix x are called the eigenvectors which correspond to the eigenvalues. The eigenvalues represent the amount of variance defined by the eigenvector. Thus, EOF x_1 defines the amount

of variance of the value γ_1 (Resio et al 1973). The table of the EOFs corresponding variance percentages is shown below and is followed contours of the 15 EOFs.

Table of Percentage of Variation each Eigenvector defines:

EIG(n)	Variance	Cumulative V
1	38.999	38.999
2	18.615	57.614
3	12.595	70.209
4	7.027	77.236
5	5.654	82.89
6	3.54	86.43
7	2.712	89.142
8	1.88	91.022
9	1.576	92.598
10	1.262	93.86
11	1.091	94.951
12	0.861	95.812
13	0.626	96.438
14	0.581	97.019
15	0.462	97.482

Contours of Eigen vectors in order EOF1-EOF15

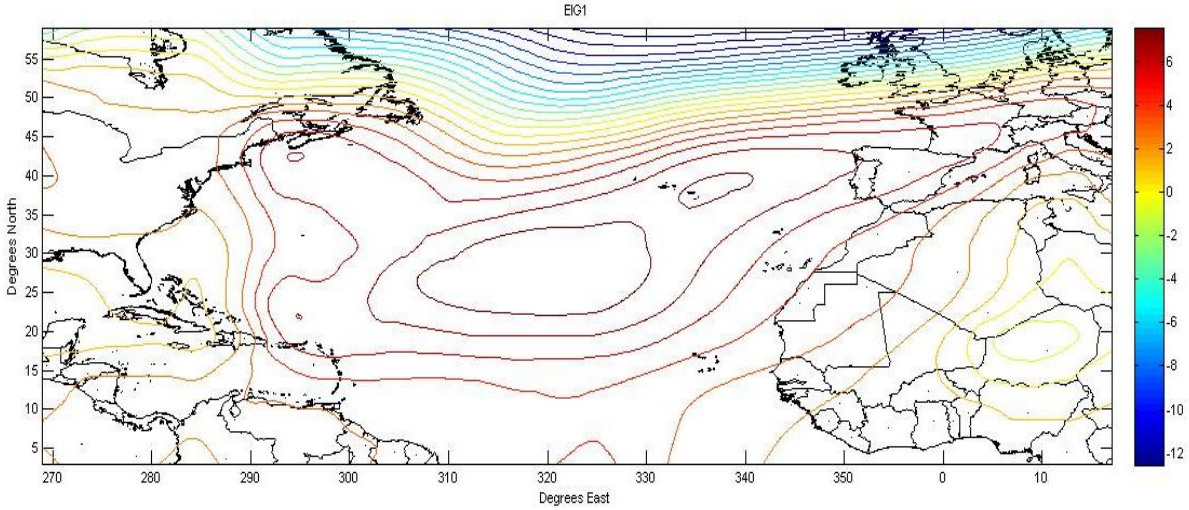

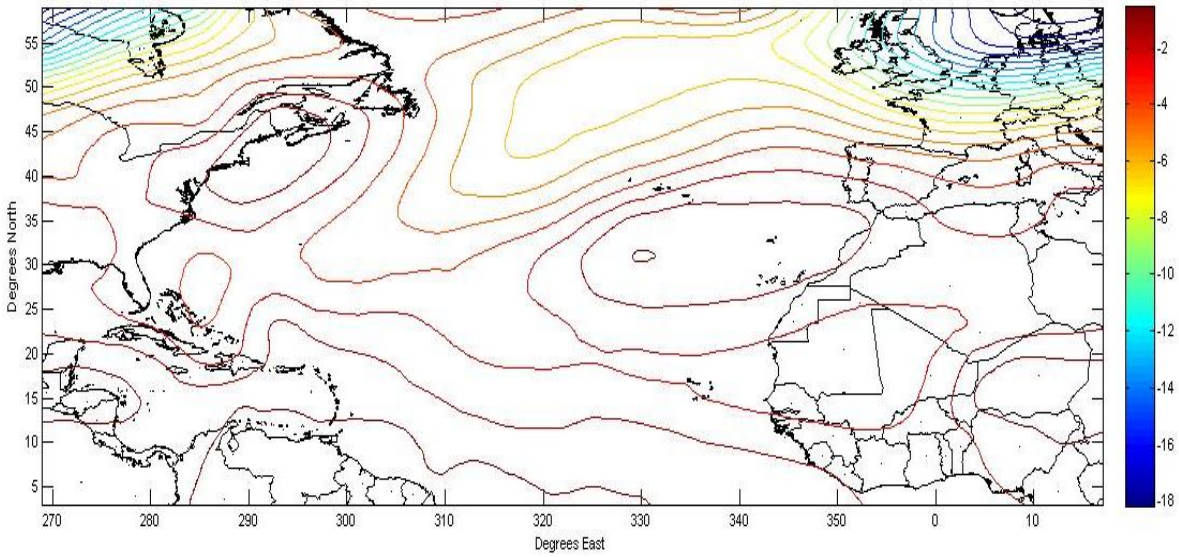
Degrees North
Degrees East
55
50
45
40
35
30
25
20
15
10
5
270
280
290
300
310
320
330
340
350
0
10
-2
-4
-6
-8
-10
-12
-14
-16
-18

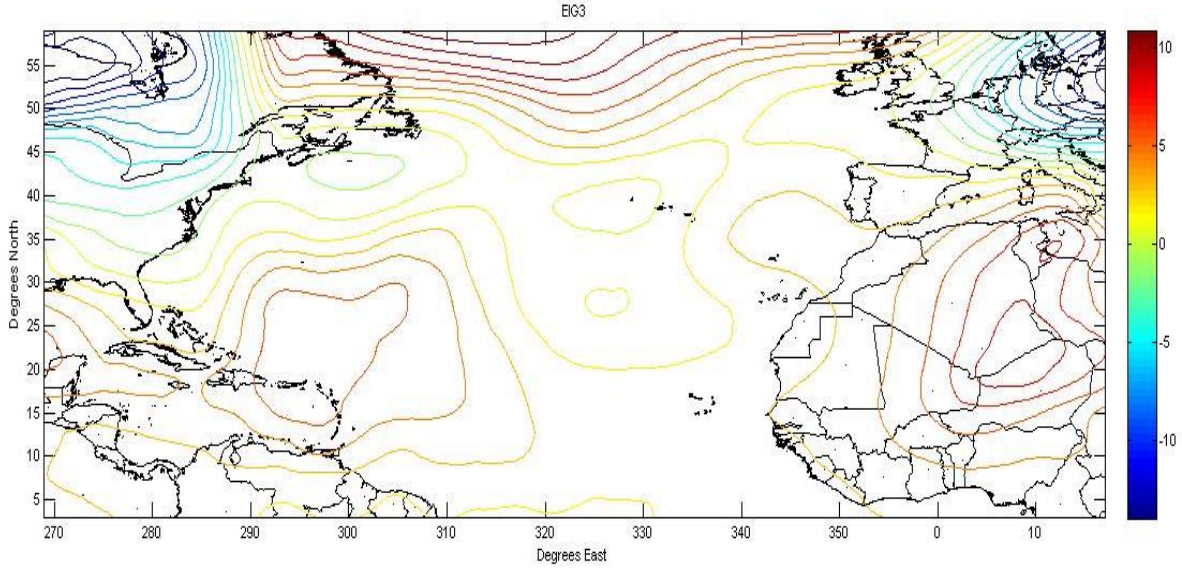
EIG3
Degrees North
Degrees East
55
50
45
40
35
30
25
20
15
10
5
270
280
290
300
310
320
330
340
350
0
10
10
5
0
-5
-10

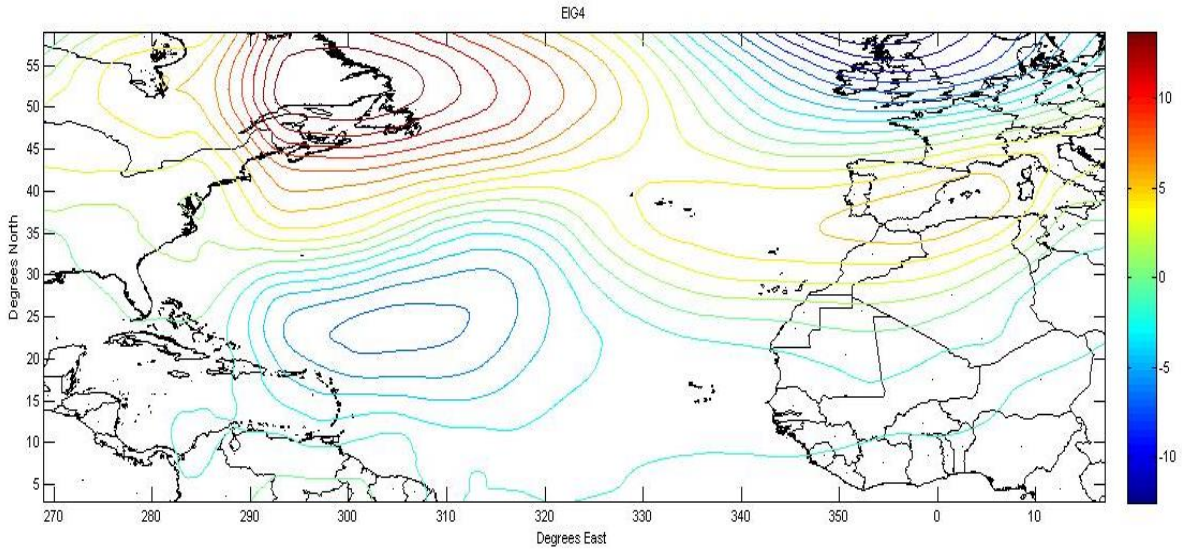
EIG4
Degrees North
Degrees East
55
50
45
40
35
30
25
20
15
10
5
270
280
290
300
310
320
330
340
350
0
10
10
5
0
-5
-10

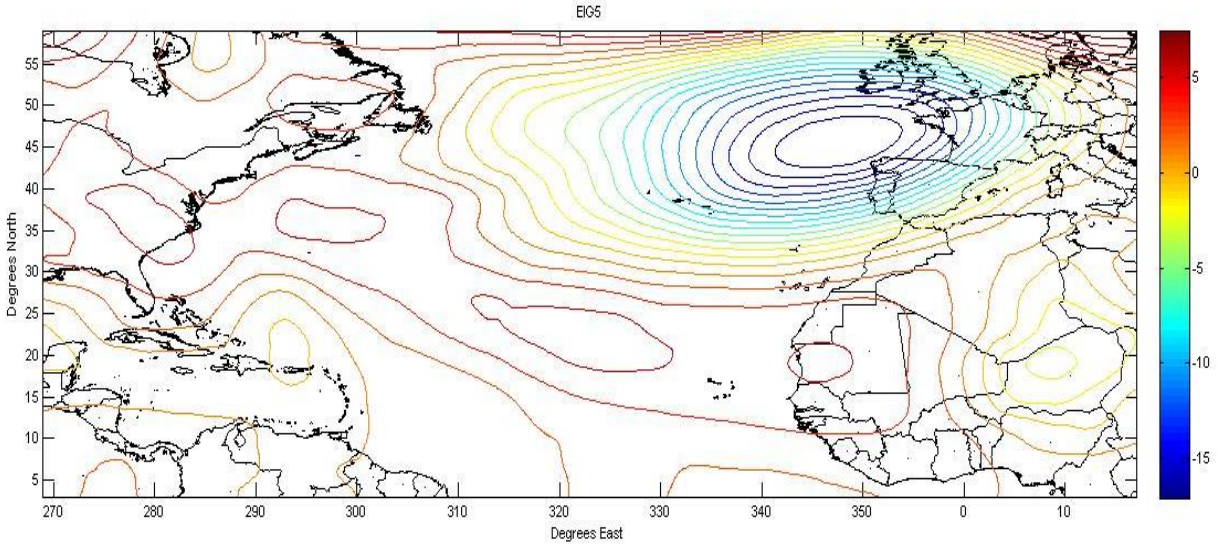
EIG5
Degrees North
Degrees East
55
50
45
40
35
30
25
20
15
10
5
270
280
290
300
310
320
330
340
350
0
10
5
0
-5
-10
-15

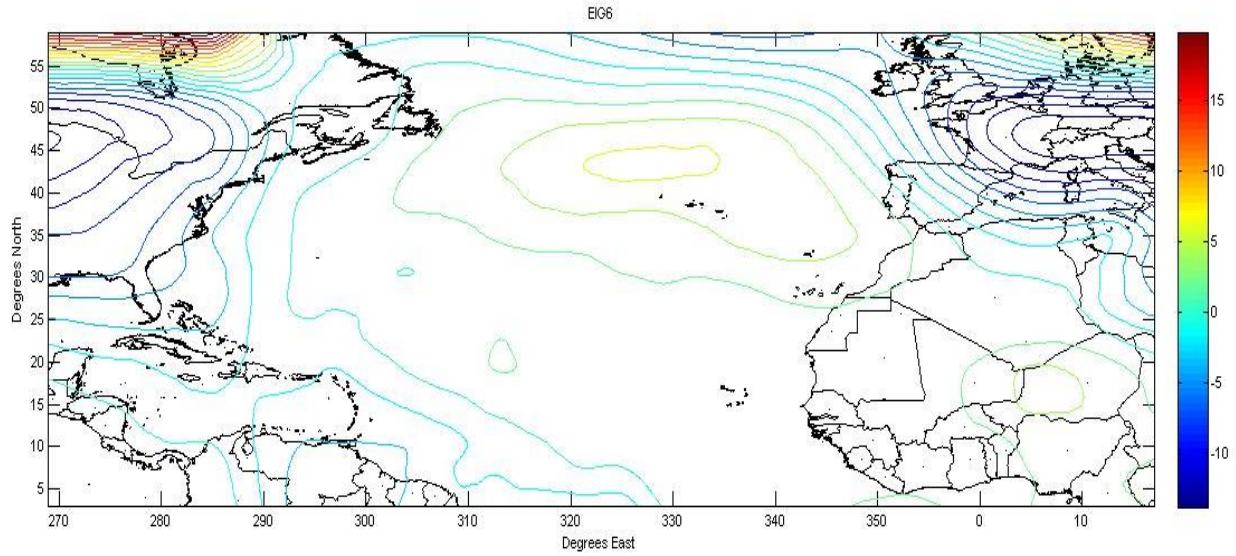
EIG6
Degrees North
Degrees East
55
50
45
40
35
30
25
20
15
10
5
270
280
290
300
310
320
330
340
350
0
10
15
10
5
0
-5
-10

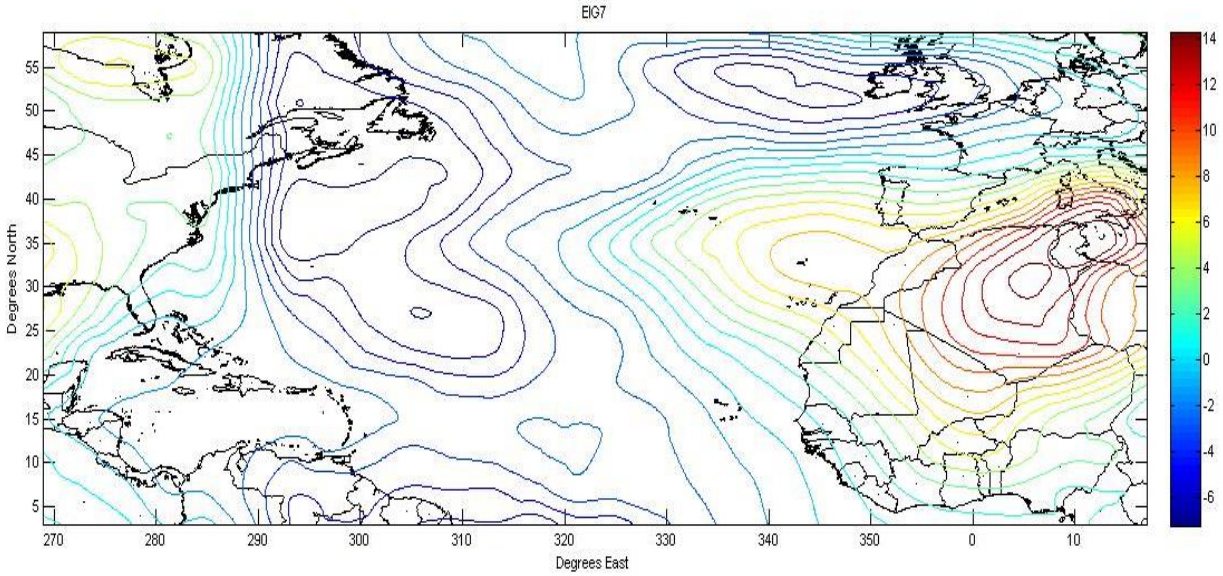
EIG7
Degrees North
Degrees East
55
50
45
40
35
30
25
20
15
10
5
270
280
290
300
310
320
330
340
350
0
10
14
12
10
8
6
4
2
0
-2
-4
-6

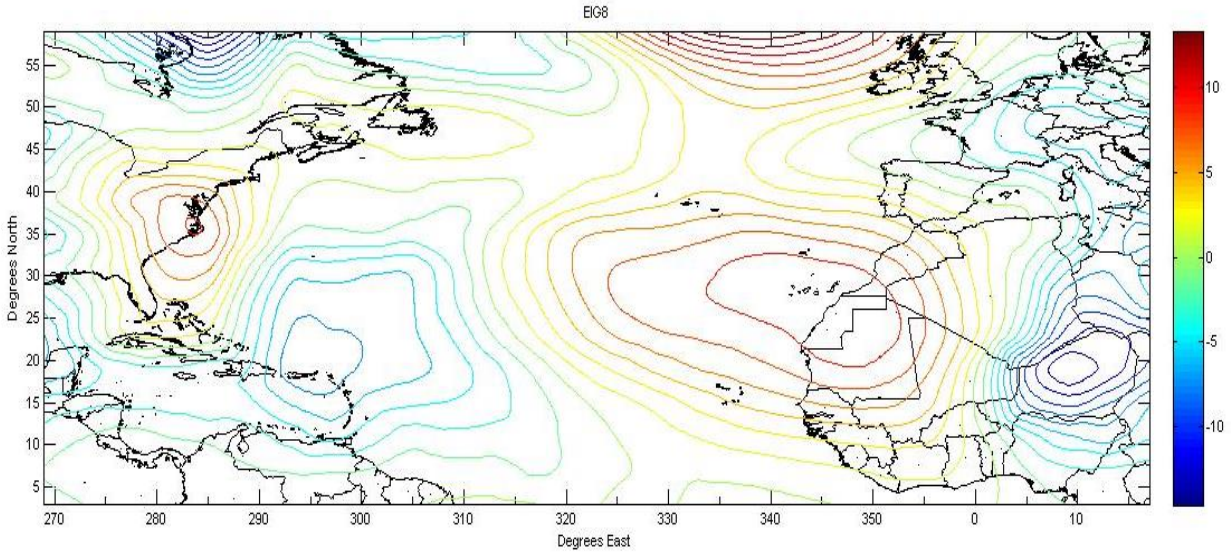
EIG8
Degrees North
Degrees East
55
50
45
40
35
30
25
20
15
10
5
270
280
290
300
310
320
330
340
350
0
10
10
5
0
-5
-10

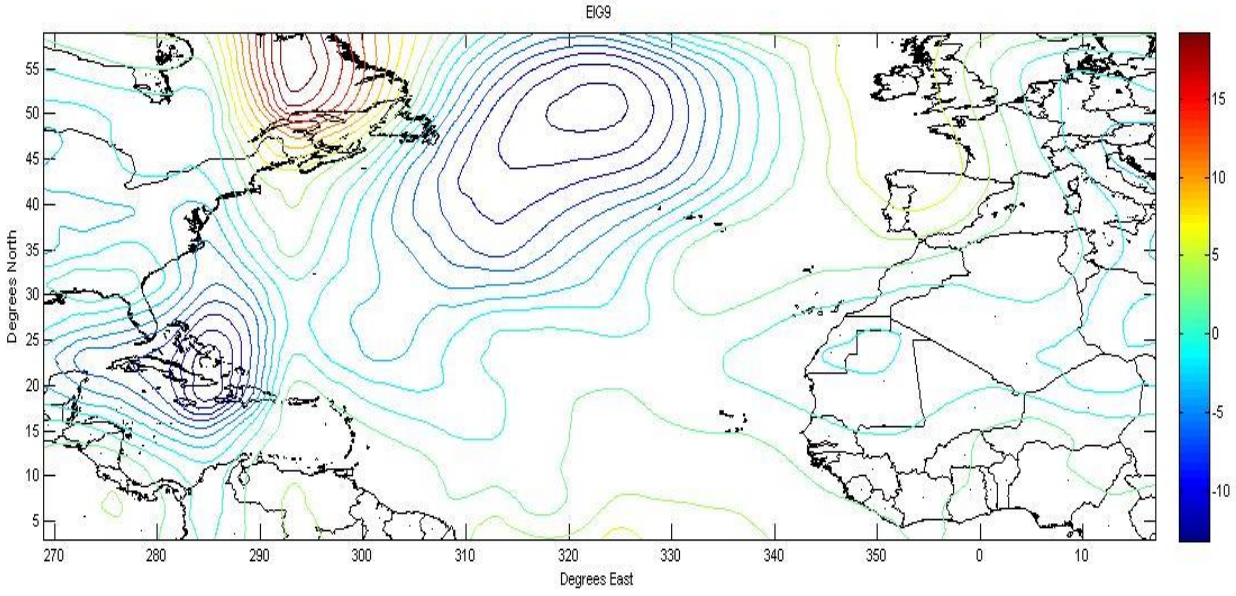
EIG9
Degrees North
Degrees East
55
50
45
40
35
30
25
20
15
10
5
270
280
290
300
310
320
330
340
350
0
10
15
10
5
0
-5
-10

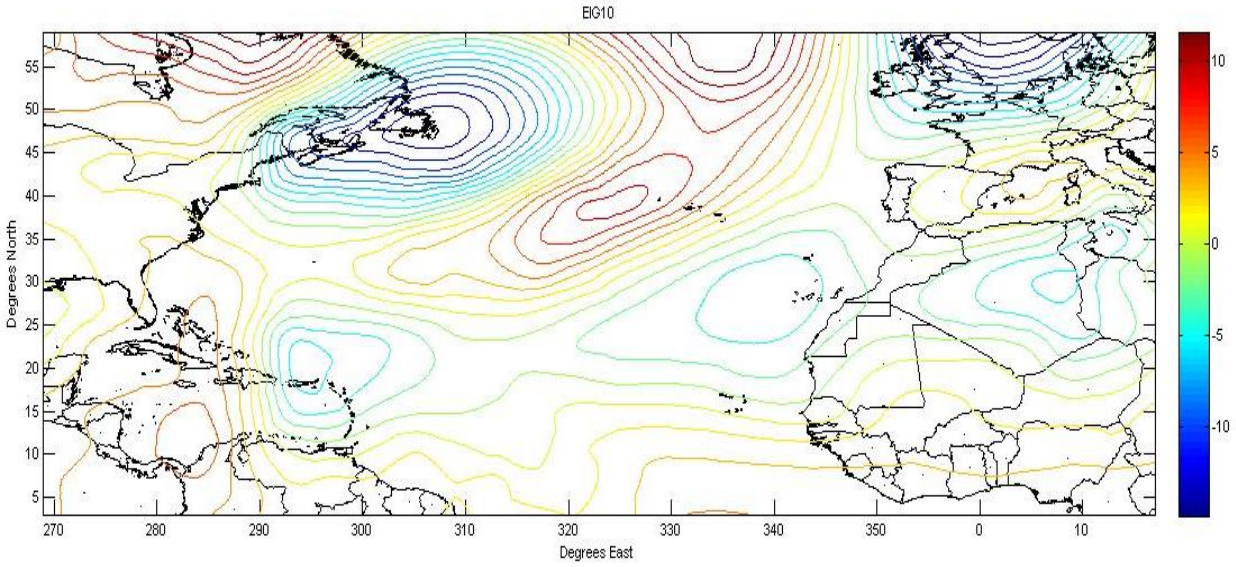
EIG10
Degrees North
Degrees East
55
50
45
40
35
30
25
20
15
10
5
270
280
290
300
310
320
330
340
350
0
10
10
5
0
-5
-10

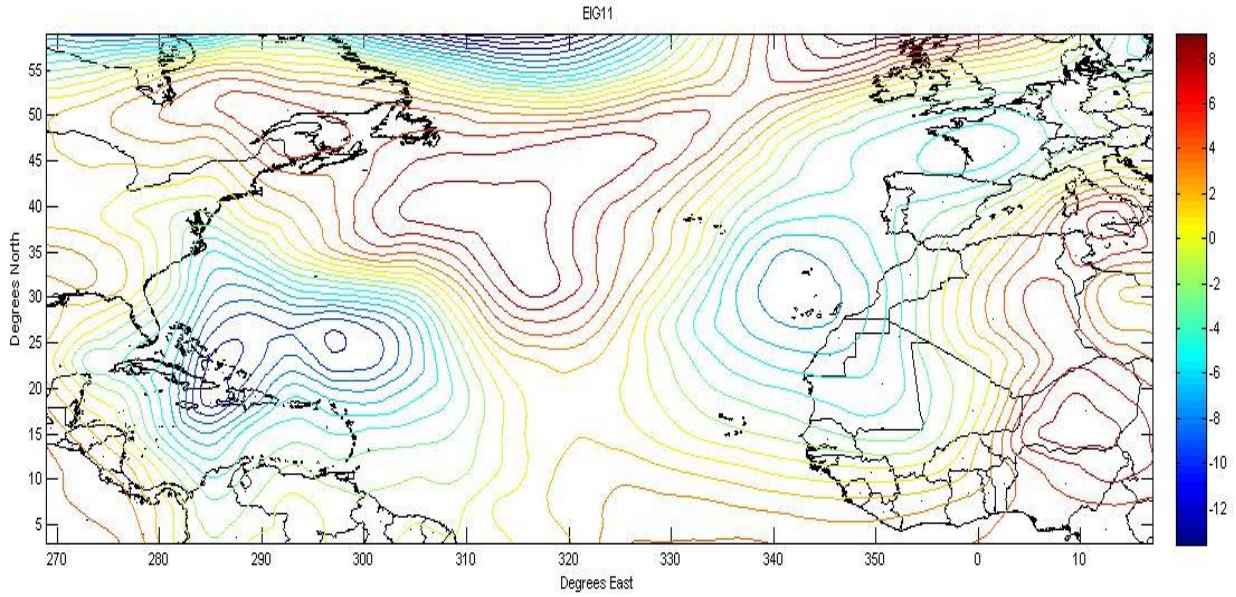
EIG11
Degrees North
Degrees East
55
50
45
40
35
30
25
20
15
10
5
270
280
290
300
310
320
330
340
350
0
10
8
6
4
2
0
-2
-4
-6
-8
-10
-12

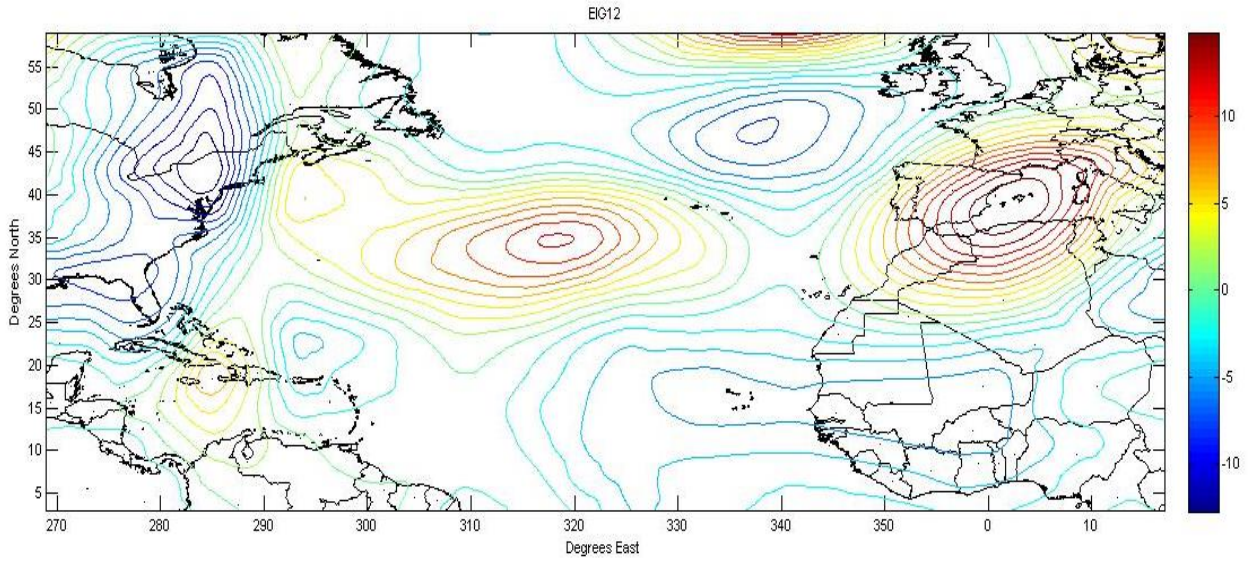
EIG12
Degrees North
Degrees East
55
50
45
40
35
30
25
20
15
10
5
270
280
290
300
310
320
330
340
350
0
10
10
5
0
-5
-10

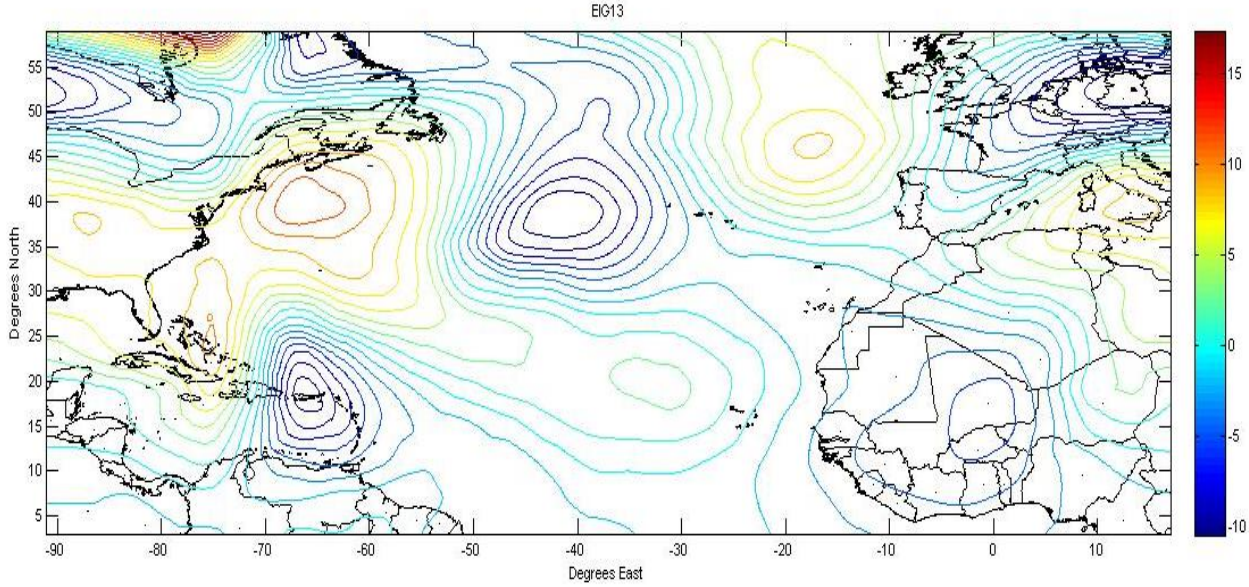
EIG13
Degrees North
Degrees East
55
50
45
40
35
30
25
20
15
10
5
-90
-80
-70
-60
-50
-40
-30
-20
-10
0
10
15
10
5
0
-5
-10

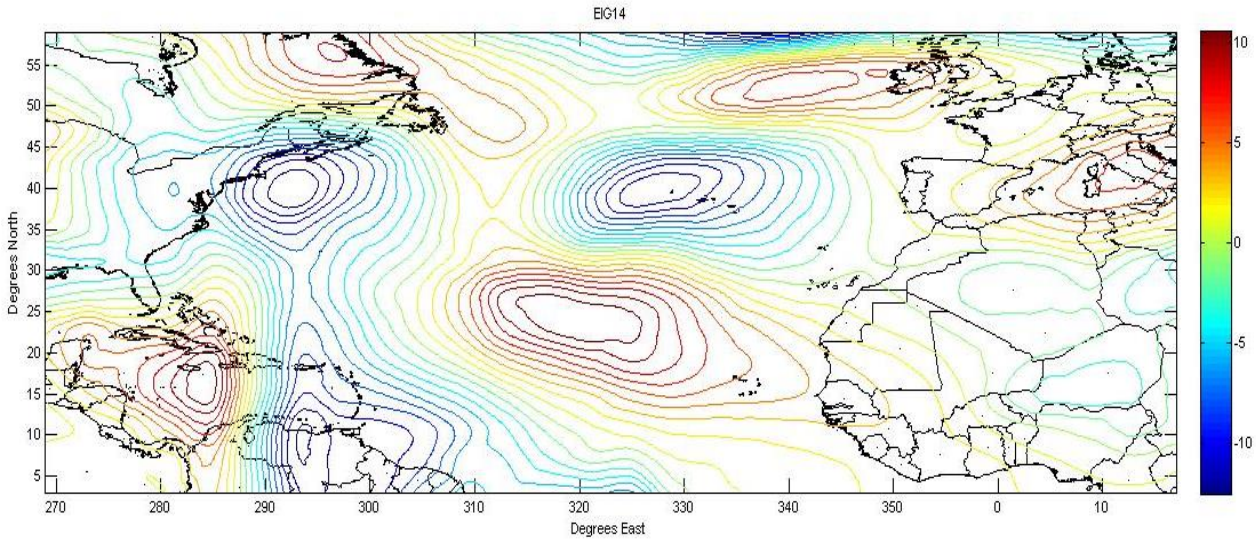
EIG14
Degrees North
Degrees East
55
50
45
40
35
30
25
20
15
10
5
270
280
290
300
310
320
330
340
350
0
10
10
5
0
-5
-10

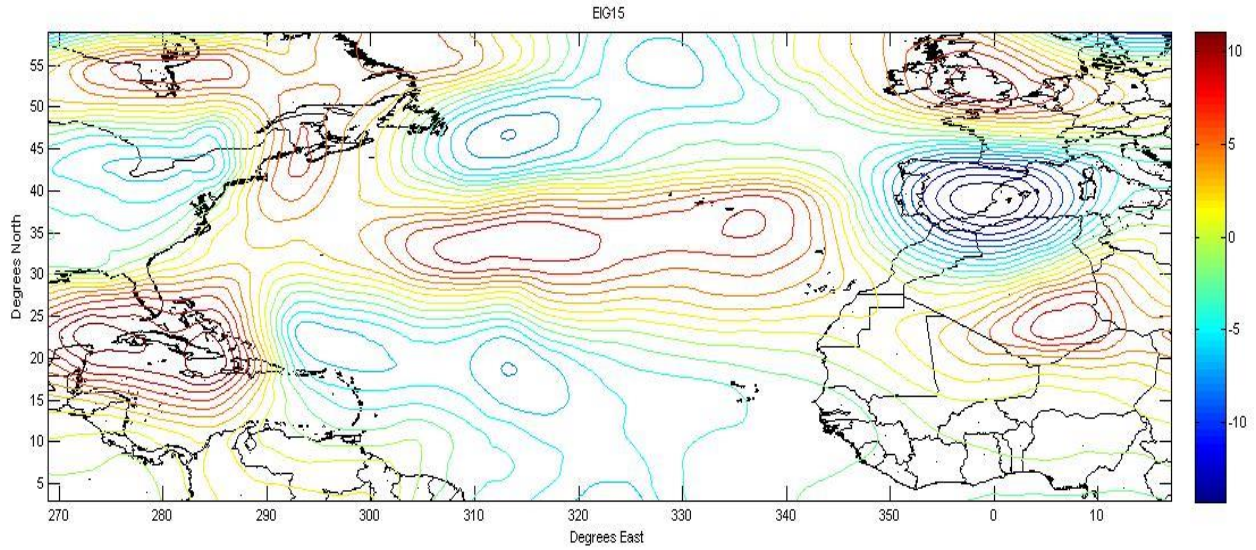
EIG15
Degrees North
Degrees East
55
50
45
40
35
30
25
20
15
10
5
270
280
290
300
310
320
330
340
350
0
10
10
5
0
-5
-10

APPENDIX B

Weightings of Eigenvectors

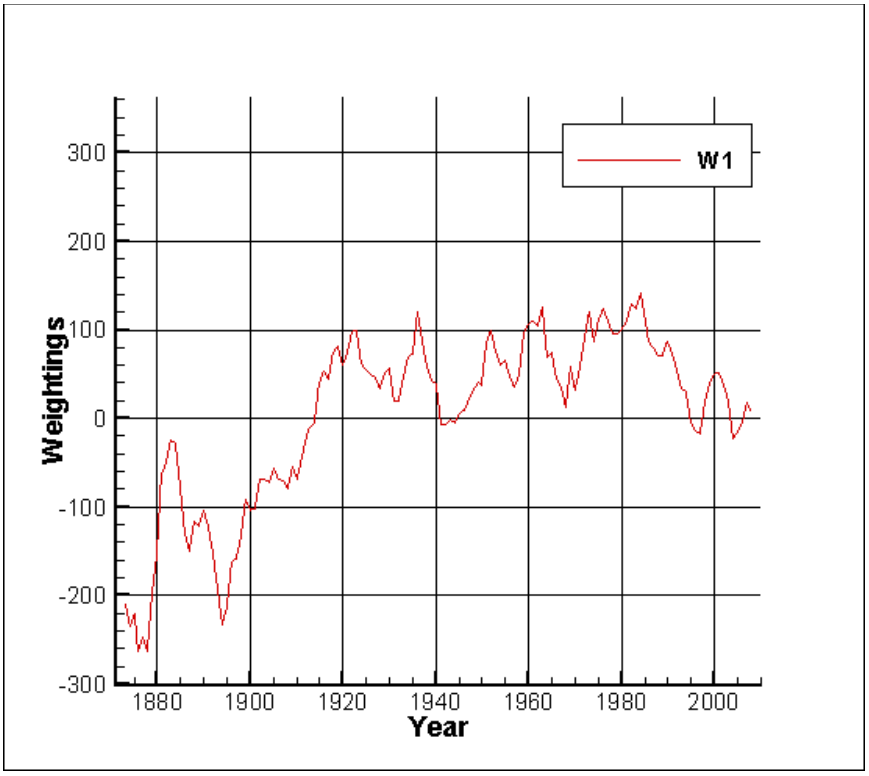

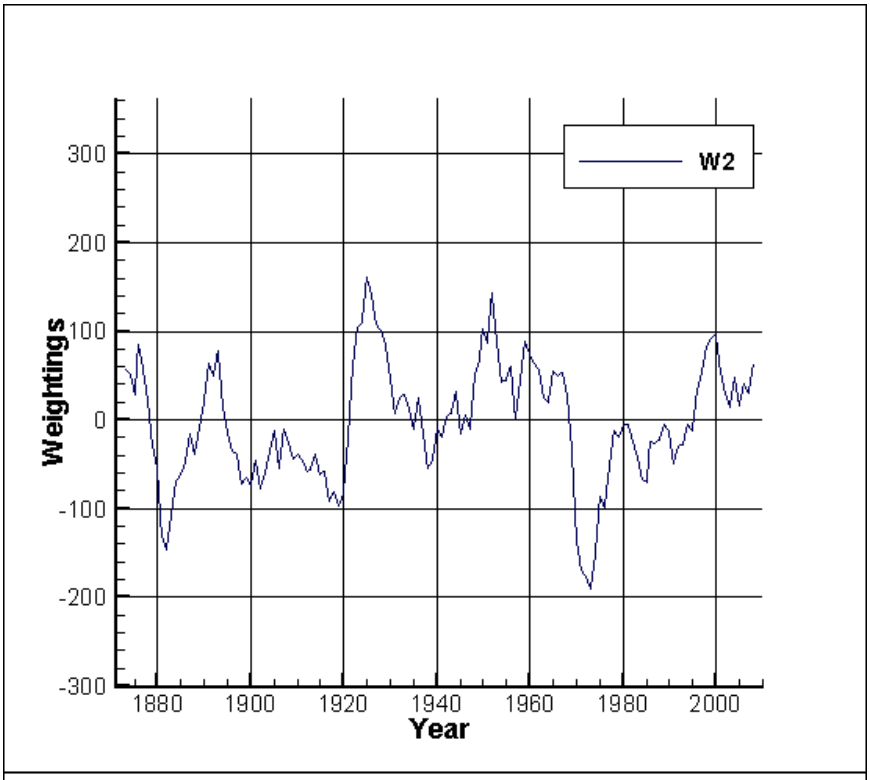
W2
300
200
100
0
-100
-200
-300
Weightings
1880
1900
1920
1940
1960
1980
2000
Year

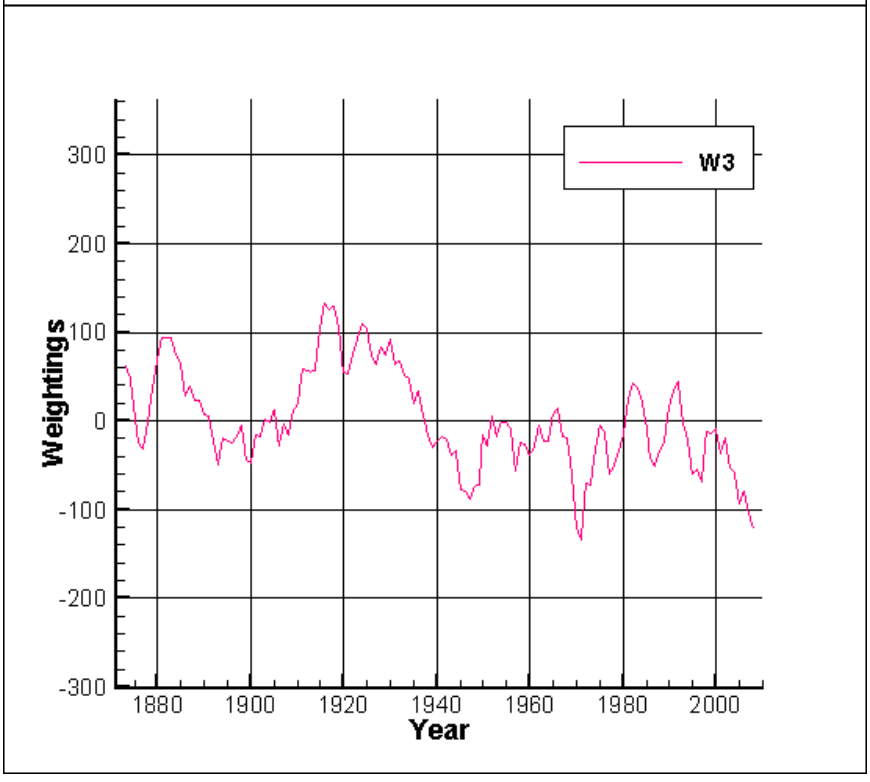
W3
300
200
100
0
-100
-200
-300
Weightings
1880
1900
1920
1940
1960
1980
2000
Year

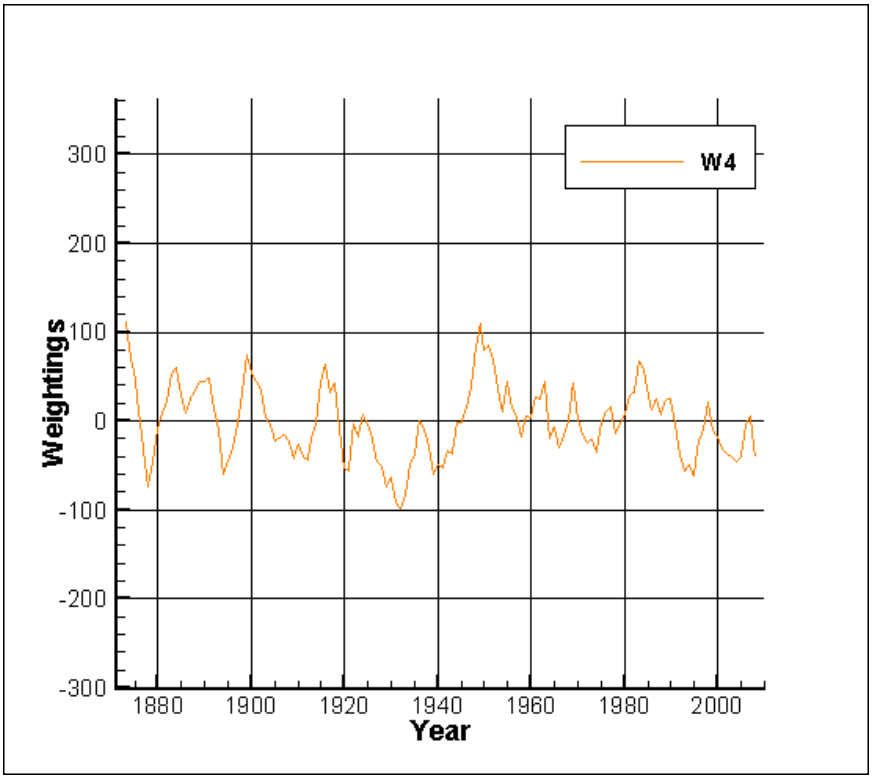
W4
300
200
100
0
-100
-200
-300
Weightings
1880
1900
1920
1940
1960
1980
2000
Year

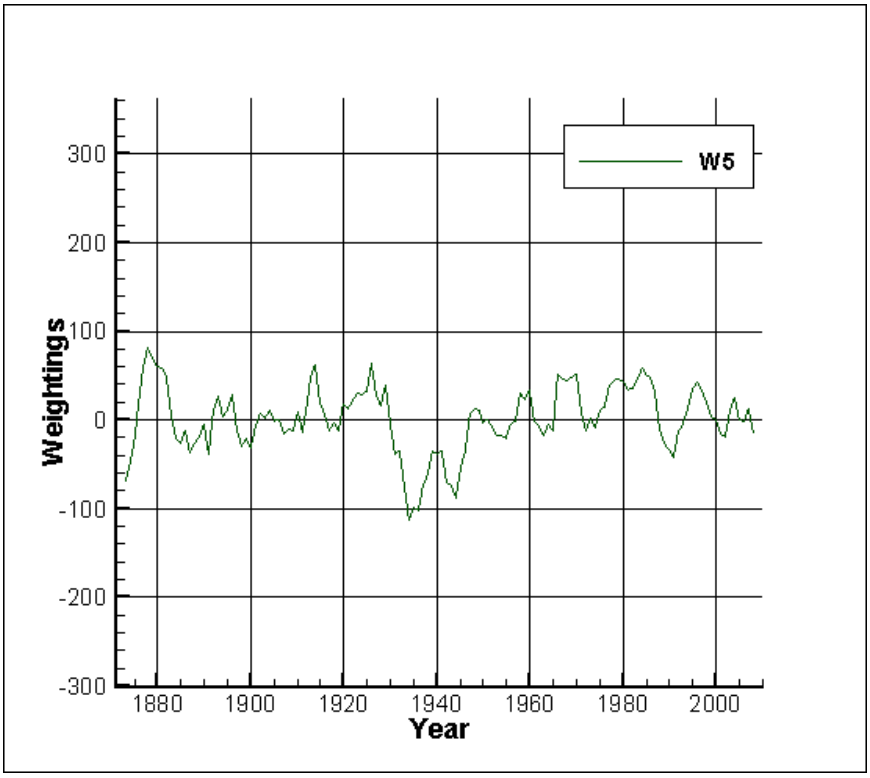
W5
300
200
100
0
-100
-200
-300
Weightings
1880
1900
1920
1940
1960
1980
2000
Year

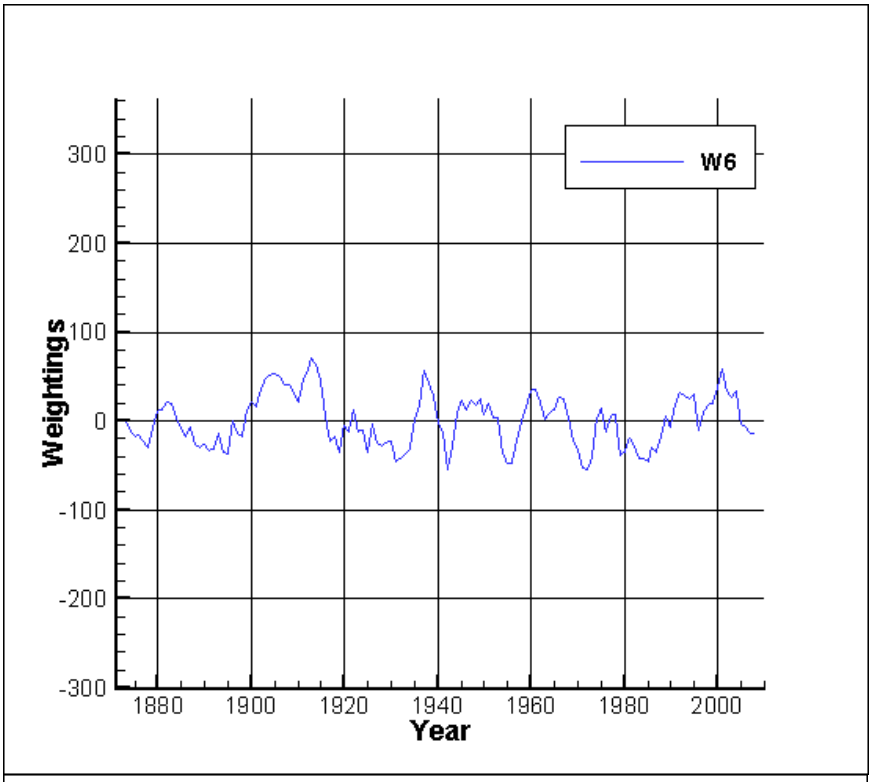
W6
300
200
100
0
-100
-200
-300
Weightings
1880
1900
1920
1940
1960
1980
2000
Year

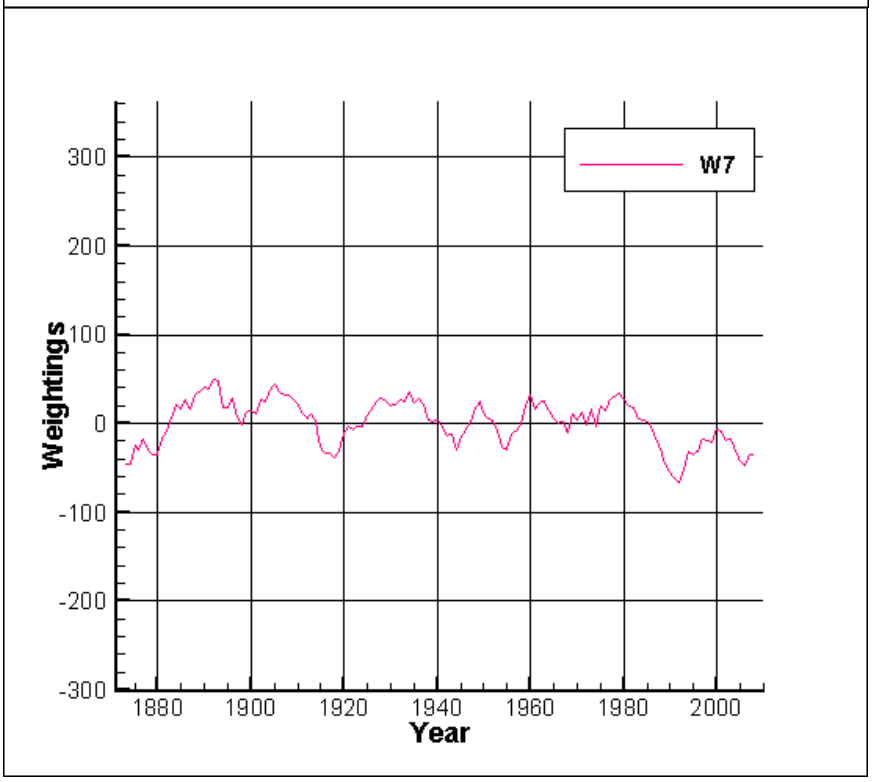
W7
300
200
100
0
-100
-200
-300
Weightings
1880
1900
1920
1940
1960
1980
2000
Year

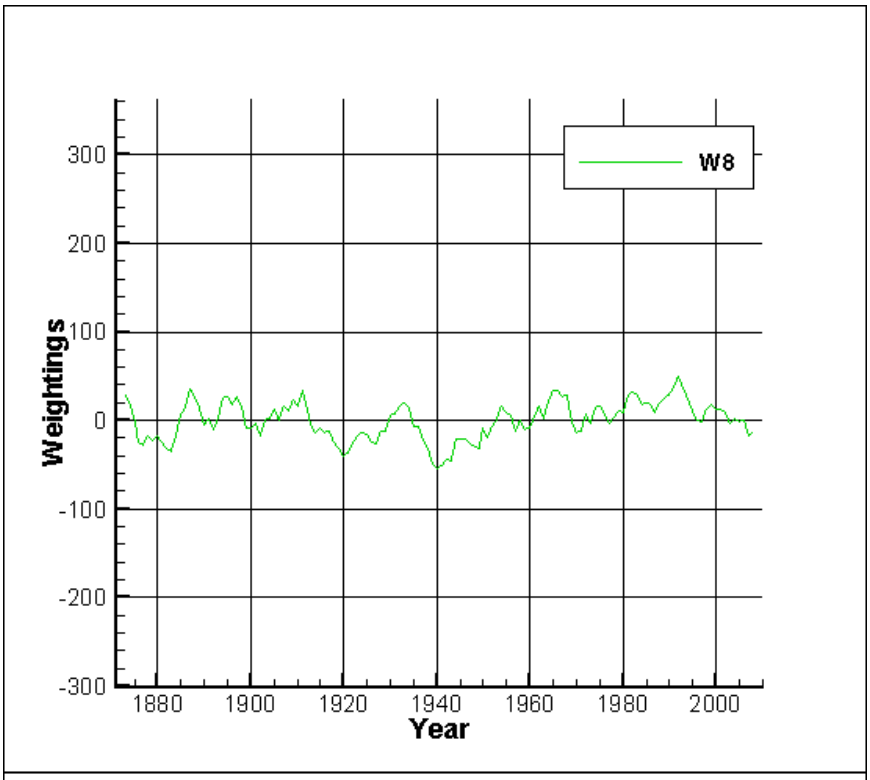
W8
300
200
100
0
-100
-200
-300
Weightings
1880
1900
1920
1940
1960
1980
2000
Year

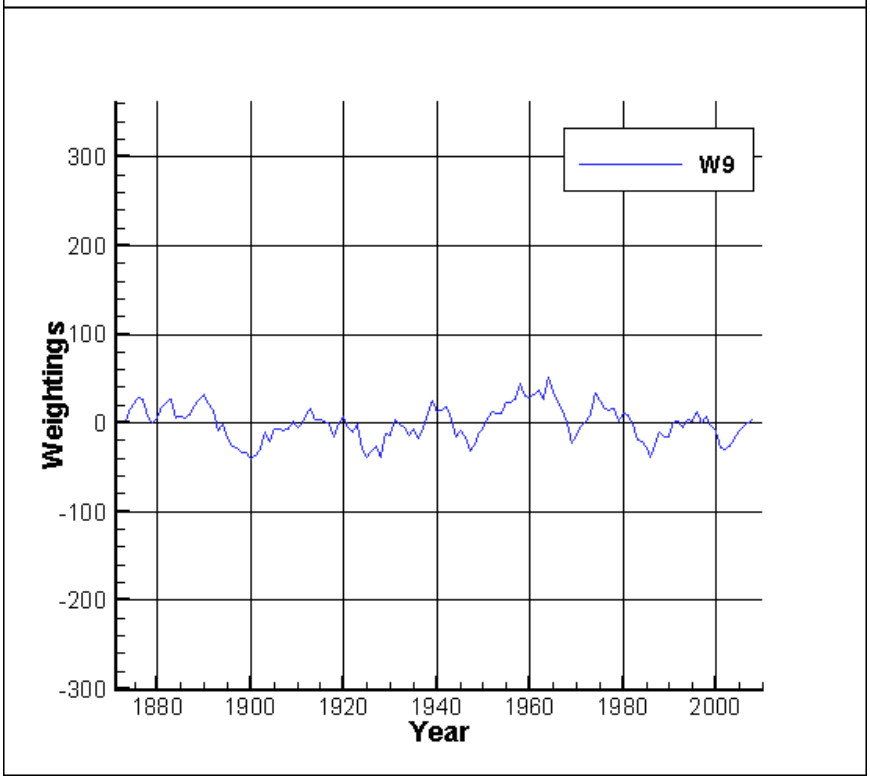
W9
300
200
100
0
-100
-200
-300
Weightings
1880
1900
1920
1940
1960
1980
2000
Year

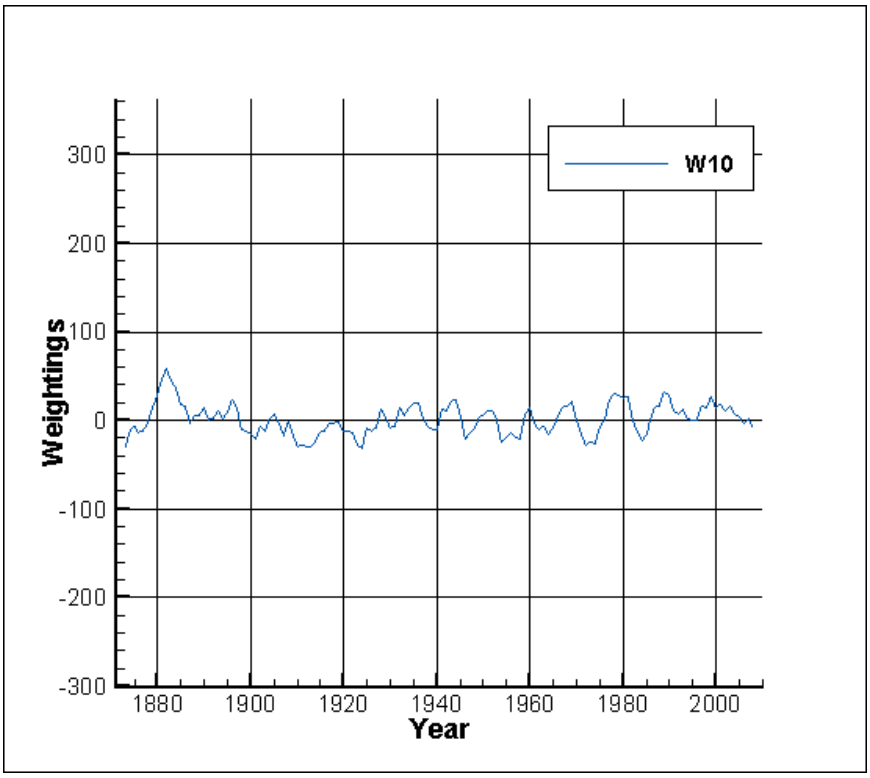

Weightings vs. SST

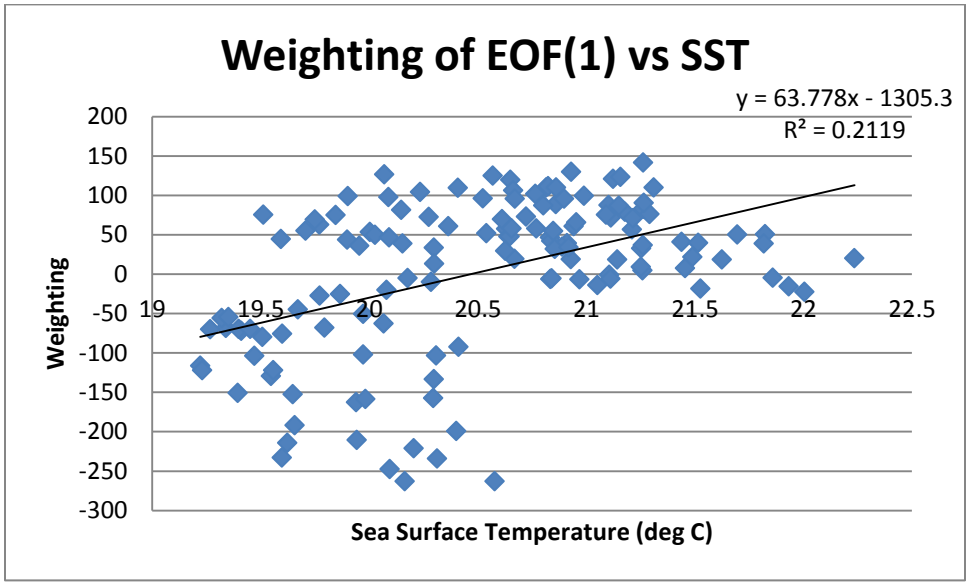

VITA

Shannon Kay, student has a Bachelor of Science in Civil Engineering from the University of North Florida, 2012 and expects to receive a Master of Science in Civil Engineering April, 2014. Dr. Donald Resio is serving as Shannon's thesis advisor. Shannon is currently employed at Manson Construction Company as an intern and will begin field engineering upon completion of school.

Shannon has ongoing interests in risk assessment, specifically for natural hazards influencing the coast and probabilistic modeling of these hazards. Shannon's academic work for this thesis includes advanced statistics and program writing using Fortran 90 as well as a basic foundation of meteorological processes.